Molecular Biology of the Cell
Vol. 12, 1061–1077, April 2001

Roles of a Fimbrin and an α-Actinin-like Protein in Fission Yeast Cell Polarization and Cytokinesis

Jian-Qiu Wu, Jürg Bähler,* and John R. Pringle†

Department of Biology and Program in Molecular Biology and Biotechnology, University of North Carolina, Chapel Hill, North Carolina 27599

Submitted September 18, 2000; Revised December 27, 2000; Accepted January 26, 2001
Monitoring Editor: Gerald R. Fink

Eukaryotic cells contain many actin-interacting proteins, including the α-actinins and the fimbrins, both of which have actin cross-linking activity in vitro. We report here the identification and characterization of both an α-actinin-like protein (Ain1p) and a fimbrin (Fim1p) in the fission yeast *Schizosaccharomyces pombe*. Ain1p localizes to the actomyosin-containing medial ring in an F-actin–dependent manner, and the Ain1p ring contracts during cytokinesis. *ain1* deletion cells have no obvious defects under normal growth conditions but display severe cytokinesis defects, associated with defects in medial-ring and septum formation, under certain stress conditions. Overexpression of Ain1p also causes cytokinesis defects, and the *ain1* deletion shows synthetic effects with other mutations known to affect medial-ring positioning and/or organization. Fim1p localizes both to the cortical actin patches and to the medial ring in an F-actin–dependent manner, and several lines of evidence suggest that Fim1p is involved in polarization of the actin cytoskeleton. Although a *fim1* deletion strain has no detectable defect in cytokinesis, overexpression of Fim1p causes a lethal cytokinesis defect associated with a failure to form the medial ring and concentrate actin patches at the cell middle. Moreover, an *ain1 fim1* double mutant has a synthetical-lethal defect in medial-ring assembly and cell division. Thus, Ain1p and Fim1p appear to have an overlapping and essential function in fission yeast cytokinesis. In addition, protein-localization and mutant-phenotype data suggest that Fim1p, but not Ain1p, plays important roles in mating and in spore formation.

INTRODUCTION

The actin cytoskeleton is involved in many processes in eukaryotic cells, including the polarization of cell growth and cytokinesis. These many roles involve the interaction of actin with a wide variety of actin-binding proteins, including proteins that can cross-link actin filaments into isotropic gels or bundles. Many actin cross-linking proteins have been purified and studied in vitro, but their functions in vivo remain poorly understood (reviewed by Matsudaira, 1994a; Otto, 1994; Furukawa and Fechheimer, 1997; Ayscough, 1998; Bartles, 2000).

Among the actin cross-linking proteins, one of the best characterized is α-actinin. It was first isolated from rabbit skeletal muscle (Ebashi and Ebashi, 1965) and has subsequently been identified in both muscle and nonmuscle cells from a variety of animals, in *Acanthamoeba*, and in *Dictyostelium* (Furukawa and Fechheimer, 1997; Critchley and Flood, 1999). α-Actinin forms a homodimer of antiparallel polypeptides (Critchley and Flood, 1999; Djinovic-Carugo *et al.*, 1999), with the actin-binding domain of each polypeptide close to the NH_2 terminus, followed by four spectrin-like repeats and two COOH-terminal EF-hand motifs. Skeletal muscle isoforms are localized to the Z-disk and are not regulated by Ca^{2+}, whereas nonmuscle isoforms are localized to focal adhesions, stress fibers, and other structures and are typically regulated by Ca^{2+}. The observation that α-actinin also binds to the cytoplasmic domains of various integral-membrane proteins has suggested that it may help to link the actin cytoskeleton to the plasma membrane. In addition, the localization of α-actinin to the cleavage furrows of chick embryos (Fujiwara *et al.*, 1978), sea urchin eggs (Mabuchi *et al.*, 1985), and cultured mammalian cells (Sanger *et al.*, 1987) has suggested that it may have a role in cytokinesis. However, the nature of this role is not clear, and neither *Dictyostelium* α-actinin mutants (Schleicher *et al.*, 1988; Rivero *et al.*, 1999) nor mammalian cells microinjected with antibodies against α-actinin (Jockusch *et al.*, 1991) displayed any obvious defect in cytokinesis.

* Present address: The Sanger Center, Wellcome Trust Genome Campus, Hinxton, Cambridge, CB10 1SA, United Kingdom.
† Corresponding author. E-mail address: jpringle@email.unc.edu.
Abbreviations used: DIC, differential-interference-contrast; GFP, green fluorescent protein; Lat-A, Latrunculin A; 3HA, triple hemagglutinin epitope.

Genetic studies have also provided only limited insights into other aspects of α-actinin function in vivo. In *Drosophila*, a single gene on the X chromosome encodes both muscle and nonmuscle isoforms by alternative splicing (Fyrberg *et al.*, 1990; Roulier *et al.*, 1992). Alleles with point mutations that sharply reduce levels of muscle α-actinin allow growth to adulthood but result in abnormalities of myofibrillar organization associated with muscle weakness or paralysis (Fyrberg *et al.*, 1990; Roulier *et al.*, 1992). The phenotypes are surprisingly mild given the myofibrils' lack of a major protein of the Z disk. Moreover, even alleles that deplete all isoforms have no obvious nonmuscle phenotype; flies hemizygous or homozygous for such alleles can complete embryogenesis and differentiation of muscle and do not die until the second day of larval growth (Fyrberg *et al.*, 1990; Roulier *et al.*, 1992). Similarly, in *Dictyostelium,* inactivation of a Ca^{2+}-sensitive α-actinin confers only subtle defects (Schleicher *et al.*, 1988; Rivero *et al.*, 1999), although the phenotypic effects are somewhat more pronounced (but still nonlethal) in double mutants defective both in this α-actinin and in a second actin cross-linking protein (either ABP-120 or the 34-kDa actin-bundling protein) (Rivero *et al.*, 1996, 1999). Taken together, the available data suggest that α-actinin might be redundant or overlapping in function with other proteins, but the identities of the redundant proteins and the degree of redundancy remain unclear.

Another well characterized actin cross-linking protein is fimbrin, a monomeric protein with two tandem α-actinin-type actin-binding motifs but no spectrin-like repeats; most fimbrins also have two EF-hand motifs at their NH_2 termini (reviewed by Matsudaira, 1994a; Otto, 1994; Ayscough, 1998; Correia and Matsudaira, 1999). Fimbrins have been identified in budding yeast, ciliates, slime molds, plants, and a variety of animals. The *Saccharomyces cerevisiae* fimbrin, Sac6p, localizes to actin cables and patches (Drubin *et al.*, 1988; Doyle and Botstein, 1996). A *sac6* null mutant has a mild phenotype on synthetic medium but has more pronounced abnormalities on rich medium (Adams *et al.*, 1991, 1993). At 23°C, it is viable with a reduced growth rate (variable in different genetic backgrounds), and the cells are rounder than wild-type cells. At 37°C, the mutant is inviable, and many cells appear lysed. Moreover, the mutant cells display defective actin cables and aberrant, mislocalized actin patches (Adams *et al.*, 1991). *Dictyostelium* fimbrin also localizes to certain actin-rich regions of the cell (Prassler *et al.*, 1997), but a mutant lacking fimbrin has no detectable defect in cytokinesis and is capable of completing development (Prassler and Gerisch, personal communication). Thus, fimbrin function may also overlap with that of other actin-binding proteins. Three human fimbrins (also called plastins) have been identified that differ in their patterns of tissue-specific expression (reviewed by Matsudaira, 1994a). Two of these proteins can substitute for Sac6p in vivo, indicating that at least some fimbrin functions have been highly conserved during evolution (Adams *et al.*, 1995). It is not yet clear whether fimbrins function in cytokinesis. The *sac6* mutant does not display an obvious cytokinesis defect, and, except in *Tetrahymena* (Watanabe *et al.*, 1998, 2000), fimbrins have not been reported to concentrate in cleavage furrows.

The fission yeast *Schizosaccharomyces pombe* provides a simple, genetically tractable model system for studies of the function of the actin cytoskeleton in cellular morphogenesis and cytokinesis (Marks and Hyams, 1985; Nurse, 1994; Chang and Nurse, 1996; Gould and Simanis, 1997; Naqvi *et al.*, 1999). During vegetative growth, the cylindrical *S. pombe* cell grows only at its poles. Immediately after cell division, only the preexisting pole (the "old end") grows; later, after "New End Take Off," both poles grow (Mitchison and Nurse, 1985). These growth patterns reflect the distribution of actin in the cell: actin cables generally run along the long axis of the cell, and cortical actin patches are concentrated at the growing pole or poles. During mitosis, growth at the cell poles ceases as the actin cytoskeleton reorganizes in preparation for division. A medial ring containing actin and a variety of associated proteins forms at the cell middle and eventually contracts during cytokinesis, and the actin patches also become concentrated at the cell middle, where they presumably contribute to the localized cell wall growth that forms the septum. During mating and sporulation, the actin cytoskeleton also undergoes rearrangements that suggest roles in various stages of the sexual cycle (Petersen *et al.*, 1998). The rearrangements of the actin cytoskeleton during the life cycle are likely to involve actin cross-linking proteins, but little information on such proteins has been available. In this article, we describe the identification and characterization of both an α-actinin–like protein (Ain1p) and a fimbrin (Fim1p) in *S. pombe.* These proteins appear to have overlapping functions during cytokinesis, and Fim1p appears to be involved also in the polarization of vegetative cells, in mating, and in sporulation.

MATERIALS AND METHODS

Strains, Growth Conditions, and Genetic and Molecular Biology Methods

The *S. pombe* strains used in this study are listed in Table 1 and/or described where appropriate below; all of them are congenic to strain 972 (Leupold, 1970). Standard growth media (YES rich medium and EMM minimal medium) and genetic methods (Moreno *et al.*, 1991) were used except where noted. Some solid media contained 2.5 μg/ml phloxin B, which accumulates in dead cells (Moreno *et al.*, 1991). SPA mating and sporulation medium contained 10 g/l glucose, 1 g/l KH_2PO_4, 1 ml/l 1000× vitamin stock solution (as used for EMM), and 30 g/l agar. For transformation, cells were grown to ~10^7 cells/ml in YES medium and then transformed using a lithium-acetate method (Bähler *et al.*, 1998b). For morphological observations and other experiments, cultures were grown overnight and maintained in mid-exponential phase (2×10^6 to 10^7 cells/ml) at the appropriate temperatures. For regulating the expression of genes under the control of the *nmt1* promoter, inducing conditions were EMM medium, and repressing conditions were either EMM containing 5 μg/ml thiamine (all experiments except where noted) or YES medium. The *nmt1* promoter begins to transcribe ~10 h after the removal of thiamine and reaches maximal steady-state levels ~6 h later (Maundrell, 1990). Growth rates were determined by measuring the OD_{595} of mid-exponential cultures at two time points at least 2 h apart. Standard recombinant-DNA methods (Sambrook *et al.*, 1989) were used except where noted. DNA was extracted from *Escherichia coli* and isolated from agarose gels using Qiagen kits (Qiagen, Santa Clarita, CA). DNA was sequenced by the UNC-CH Automated Sequencing Facility on a Model 373A DNA Sequencer with the *Taq* DyeDeoxy Terminator Cycle Sequencing kit (Applied Biosystems, Foster City, CA). Oligonucleotide primers were obtained from Integrated DNA Technologies (Coralville, IA).

Table 1. *S. pombe* strains used in this study

Strain	Genotype	Source/Reference
972	*h*$^-$ wild type	Leupold, 1970
975	*h*$^+$ wild type	Leupold, 1970
JW9	*h*$^-$/*h*$^+$ *ade6-M210/ade6-M216 leu1-32/leu1-32 ura4-D18/ura4-D18*	This study[a]
JW34	*h*$^-$ *41nmt1-GFP-ain1*$^+$	See text
JW35	*h*$^-$ *81nmt1-GFP-ain1*$^+$	See text
JW46	*h*$^-$ *ain1*$^+$*-GFP*	See text
JW52	*h*$^+$ *ain1*$^+$*-GFP*	JW46 × 975
JW49	*h*$^-$ *3nmt1-ain1*$^+$	See text
JW45	*h*$^-$ *ain1-Δ1*	See text
JW53	*h*$^+$ *ain1-Δ1*	JW45 × 975
JW106	*h*$^-$ *fim1*$^+$*-3HA*	See text
JW109	*h*$^-$ *fim1*$^+$*-GFP*	See text
JW117	*h*$^+$ *fim1*$^+$*-GFP*	JW109 × 975
JW144	*h*$^-$ *fim1-Δ1 ade6 leu1-32 ura4-D18*	See text
JW142	*h*$^+$ *fim1-Δ1*	JW144 × 975
JW110	*h*$^-$ *3nmt1-fim1*$^+$	See text
JW111	*h*$^-$ *41nmt1-fim1*$^+$	See text
JW113	*h*$^-$ *3nmt1-GFP-fim1*$^+$	See text
JW164	*ain1-Δ1 41nmt1-fim1*$^+$	JW53 × JW111
KGY1010	*h*$^-$ *act1-48 leu1-32 lys1-131 ura4-D18*	McCollum *et al*., 1996
YDM74	*h*$^-$ *myo2-E1 ade6 his3-D1 leu1-32 ura4-D18*	D. McCollum[b]
JW21	*h*$^+$ *cdc4-8*	P. Nurse (Nurse *et al*., 1976; McCollum *et al*., 1995)
JB24	*h*$^-$ *cdc3-6*	P. Nurse (Nurse *et al*., 1976; Balasubramanian *et al*., 1994)
YDM136	*h*$^-$ *cdc8-110 his3-D1 leu1-32 ura4-D18*	D. McCollum (Balasubramanian *et al*., 1992)
YDM26	*h*$^-$ *rng2-D5 ade6 leu1-32 ura4-D18*	D. McCollum (Eng *et al*., 1998)
MBY310	*h*$^+$ *cdc12-112 ade6-M210 leu1-32 ura4-D18*	K.L. Gould (Chang *et al*., 1997; Eng *et al*., 1998)
JB41	*h*$^-$ *mid1-ΔF ade6-M216 leu1-32 ura4-D18*	V. Simanis (Sohrmann *et al*., 1996)
JB110	*h*$^-$ *pom1-Δ1 ura4-D18*	Bähler and Pringle, 1998
JB23	*h*$^-$ *cdc14-118 leu1-32*	P. Nurse (Nurse *et al*., 1976)[c]
JW124	*h*$^+$ *cdc16-116 ade6-M210 leu1-32 ura4-D18*	K.L. Gould (Minet *et al*., 1979)[c]
YDM188	*h*$^-$ *arp3-c1 ade6-M210 leu1-32 ura4-D18*	McCollum *et al*., 1996
JB30	*h*$^-$ *nda3-KM311 leu1-32*	Hiraoka *et al*., 1984

[a] Derived by mating two haploid strains obtained from J. Kohli.

[b] *myo2-E1* was originally referred to as *rng5-E1* (Balasubramanian *et al*., 1998; Eng *et al*., 1998).

[c] See also Gould and Simanis (1997) and references cited therein.

Deletion and Tagging of ain1

ain1 was deleted and tagged in strain 972 by polymerase chain reaction (PCR)-based gene targeting (Bähler *et al*., 1998b) using *kanMX6*, which confers resistance to G418/Geneticin (Life Technologies, Gaithersburg, MD), as the selectable marker. For deletion, the forward primer contained sequences corresponding to nucleotides −163 to −83 relative to the start codon, and the reverse primer contained sequences corresponding to the complement of nucleotides 83 to 162 downstream of the stop codon. (The adjacent genes do not impinge closely on the region deleted.) Checking by PCR (Bähler *et al*., 1998b) identified two stable G418-resistant transformants that had sustained the desired integration at the *ain1* locus. When these transformants were crossed to strain 975, all tetrads dissected produced four viable spores that segregated 2:2 for G418 resistance, indicating that the transforming DNA had integrated at a single site. One G418-resistant segregant (strain JW45) was chosen for further experiments. JW45, five other G418-resistant segregants, and the two original transformants all had the same phenotype under stress conditions (see RESULTS), suggesting that no suppressors existed in the original transformants.

To tag Ain1p at its COOH terminus with green fluorescent protein (GFP), the *ain1*-specific sequences (79 bp) of the forward primer ended just upstream of the stop codon, and the reverse primer was the same as that used for the deletion. Checking by PCR identified a G418-resistant transformant (strain JW46) that had sustained the desired integration event and segregated 2:2 for G418 resistance when crossed to strain 975. In addition, *ain1*$^+$ was placed under the control of three versions of the thiamine-regulated *nmt1* promoter (the wild-type *3nmt1*, the attenuated *41nmt1*, and the still weaker *81nmt1*) (Basi *et al*., 1993; Forsburg, 1993), with or without an associated NH_2-terminal GFP tag (Bähler *et al*., 1998b). The *ain1*-specific sequences (70 bp) of the forward primer corresponded to nucleotides −163 to −94, and those (76 or 70 bp) of the reverse primers corresponded to the complement of the NH_2-terminal codons. Checking by PCR identified G418-resistant transformants (strains JW34, JW35, and JW49) that had sustained the desired integration events and segregated 2:2 for G418 resistance when crossed to strain 975. Strains JW46, JW34 (grown under repressing conditions), and JW35 (grown under inducing conditions) all formed normal colonies and had normal cell morphology on various media and at various temperatures, including EMM + 1 M KCl medium at 18°C, conditions under which *ain1* deletion cells are severely defective (see RESULTS). In addition, although the *ain1-Δ1 fim1-Δ1* double mutant was synthetically lethal at 25°C (see RESULTS), an *ain1*$^+$*-GFP fim1-Δ1* strain was viable and resembled *fim1-Δ1* single-mutant cells in cell morphology. Thus, both Ain1p-GFP and GFP-Ain1p appear to provide normal Ain1p function.

```
-225 TTTTTACAAT TGCAAATTAA CTTTTAACAG ATTGGCTAAG CAAACGTGTA

-175 TTAACTCATT TAGCGAGCGG ATCAAAGTTT TGCTCTACGC TTCTGTAAGT

-125 ATGATGTATGT GCATCAACA ACACGACGTT AATCCTTGTC ACGTAGCAAC

-75  TGCAAGCCAC CCAAAGCACA CATCGTGTGG TTTCGTTTAC TATACATTTT
                             *  *  *
-25  TTGGTCAAAT TTTACTTTTA AAGAAATGTT AGCTCTTAAA CTTCAAAAGA
```

Figure 1. Identification of the *fim1* start codon (see text for details). The putative start codon is underlined and in boldface; an upstream ATG (−125 to −123) is in boldface; the possible intron donor and acceptor sequences are underlined; and the 5′ ends of the three cDNAs are underscored by *.

Cloning, Deletion, and Tagging of fim1

fim1 sequences were amplified by PCR with degenerate primers that corresponded to two regions conserved among eight fimbrins known at the time (see Figure 2B). The forward primer (5′-CCNGAYACNATHGAYGARMG-3′, where N = A, C, G, or T; Y = C or T; H = A, C, or T; R = A or G; M = A or C) encoded the peptide PDTIDER and was 768-fold degenerate, and the reverse primer (5′-ACRAANGCNARRTTNARYTT-3′) was the complement of the sequence encoding the peptide KLNLAFV and was 2048-fold degenerate. *Taq* polymerase (Promega, Madison, WI) was used as recommended by the supplier, and DNA from an *S. pombe* genomic-DNA library (a gift from P. Young, Queens University, Ontario, Canada) constructed in the plasmid pWH5 (Wright *et al.*, 1986) was used as template. After denaturing the template for 5 min at 94°C, 38 cycles of 94°C for 1 min, 50°C for 1.5 min, and 72°C for 1 min were performed followed by a 10-min extension at 72°C. A major PCR product of ~580 bp was obtained and cloned into the pGEM-T Easy vector (Promega), and sequencing of the cloned fragment revealed that it would encode a peptide of 192 amino acids that was 77 and 47% identical to the corresponding regions of *S. cerevisiae* Sac6p and human L-plastin, respectively. The cloned fragment was then used to screen the pWH5 library by colony hybridization. Plasmid pG16–2 was isolated and sequenced; it appeared to contain a complete fimbrin coding sequence (designated *fim1*) interrupted (at positions 235 to 310 and 1800 to 1853 relative to the A of the putative initiation codon) by two introns with conserved donor, splice-branch, and acceptor sequences. To confirm the presence of these introns, the absence of other introns within the *fim1* coding region, and the identification of the putative start and stop codons, cDNA sequences were amplified by PCR using the Expand High Fidelity System (Boehringer Mannheim, Indianapolis, IN), one or the other of two cDNA libraries as template, and primers corresponding to *fim1* genomic sequences or vector sequences. One library (kindly provided by Dr. C. Albright, Vanderbilt University, Nashville, TN) was constructed in vector pREP3X (Basi *et al.*, 1993; Forsburg, 1993), and the other (Becker *et al.*, 1991) was constructed in vector pDB20. The PCR products were cloned into the pGEM-T Easy vector and sequenced.

In addition to the two confirmed introns, a third possible intron is present at positions −120 to −80 (Figure 1); if these sequences were removed by splicing, the ATG at positions −125 to −123 would be in frame with the rest of the coding sequence and thus might be the actual initiation codon. However, several lines of evidence argue strongly against this possibility. First, although the −120 to −80 region has consensus intron donor and acceptor sequences (Figure 1), no commonly used branch site (Prabhala *et al.*, 1992) is present. Second, removal of these sequences by splicing and initiation of translation at the −125 to −123 ATG would result in Fim1p's having 28 additional NH_2-terminal amino acids that would not correspond to the NH_2 termini of other known fimbrins (see Figure 2B). Third, three different cDNAs obtained from two different libraries (see above) all have 5′ ends between positions −54 and −48 (Figure 1). Finally, when GFP-encoding sequences were inserted at the presumed actual start codon under control of the *3nmt1* promoter (strain JW113; see below), a GFP-fimbrin fusion protein was produced that showed nearly normal fimbrin localization (see RESULTS) under repressing conditions and caused a severe defect in cytokinesis (similar to that of *3nmt1-fim1*$^+$ cells; see Figure 7A) under inducing conditions. In contrast, when the same tagging was performed at the −125 to −123 ATG, no specific GFP localization was observed under either repressing or inducing conditions, and no overexpression phenotype was observed under inducing conditions.

fim1 was deleted and tagged as described for *ain1* except that deletion was performed in the diploid strain JW9. For deletion, the forward primer contained sequences corresponding to nucleotides −116 to −17 relative to the start codon, whereas the reverse primer contained sequences corresponding to the complement of nucleotides 68 to 147 downstream of the stop codon. (The adjacent genes do not impinge closely on the region deleted.) Checking by PCR identified two G418-resistant transformants that had sustained the desired integration. Fifteen tetrads from each transformant yielded mostly three or four viable spores, and about half of the viable spores were G418-resistant (with 2:2 segregation in tetrads with four viable spores). One such segregant (strain JW144) was chosen for further experiments. To tag Fim1p at its COOH terminus with GFP or a triple hemagglutinin epitope (3HA), the forward primer contained 78 nucleotides corresponding to those just upstream of the *fim1* stop codon, and the reverse primer was the same as that used for deletion. Checking by PCR and tetrad analysis revealed G418-resistant transformants (strains JW106 and JW109) that had sustained the desired integrations. The tagged proteins appeared to be at least largely functional as judged by two criteria. First, cells of strains JW106 and JW109 formed normal colonies and resembled wild-type cells in morphology during growth on EMM medium at 36°C or on EMM + 1 M KCl medium at temperatures from 18 to 36°C, conditions under which *fim1* deletion cells had strong phenotypes (see RESULTS). Second, although the *ain1-Δ1 fim1-Δ1* double mutant was synthetically lethal (see RESULTS), strains harboring *ain1-Δ1* and either one of the tagged *fim1* genes were viable and had normal cell morphology. However, the *ain1*$^+$ *fim1*$^+$*-GFP* cells did display some morphological abnormalities during growth on rich medium at 36°C, suggesting that Fim1p-GFP was not completely normal in function.

To place *fim1*$^+$ under control of the *nmt1* promoters (with or without an NH_2-terminal GFP tag), the forward primer contained sequences corresponding to nucleotides −210 to −131 relative to the *fim1* start codon, and the reverse primers contained 77 bp corresponding to the complement of the NH_2-terminal codons. Checking by PCR revealed G418-resistant transformants (strains JW110, JW111, and JW113) that had sustained the desired integrations and segregated 2:2 for G418 resistance.

Morphological Observations and Latrunculin Treatment

Cells were observed by fluorescence or differential-interference-contrast (DIC) microscopy using a Nikon Microphot SA microscope with a 60× Plan-apo objective. To visualize overall cell morphologies or GFP signals together with septa and DNA in the same cells, cells in growth medium were double-stained by adding 1/20 volume of a 1-mg/ml stock solution (in 50 mM sodium citrate, 100 mM sodium phosphate, pH 6.0) of Calcofluor (Sigma, St. Louis, MO) and 1/125 volume of a 1-mg/ml stock solution (in water) of bisBenzimide (Sigma), and then photographed immediately. Immunofluorescence of 3HA-tagged cells was performed as described previously (Bähler and Pringle, 1998), using the monoclonal HA11 primary antibody (Berkeley Antibody, Richmond, CA) and fluorescein isothiocyanate (FITC)-tagged goat anti-mouse-IgG secondary antibody (Jackson ImmunoResearch, Laboratories, West Grove, PA). Staining of F-actin with rhodamine-phalloidin (Molecular Probes, Eugene, OR) was performed using the method of Sawin and Nurse (1998)

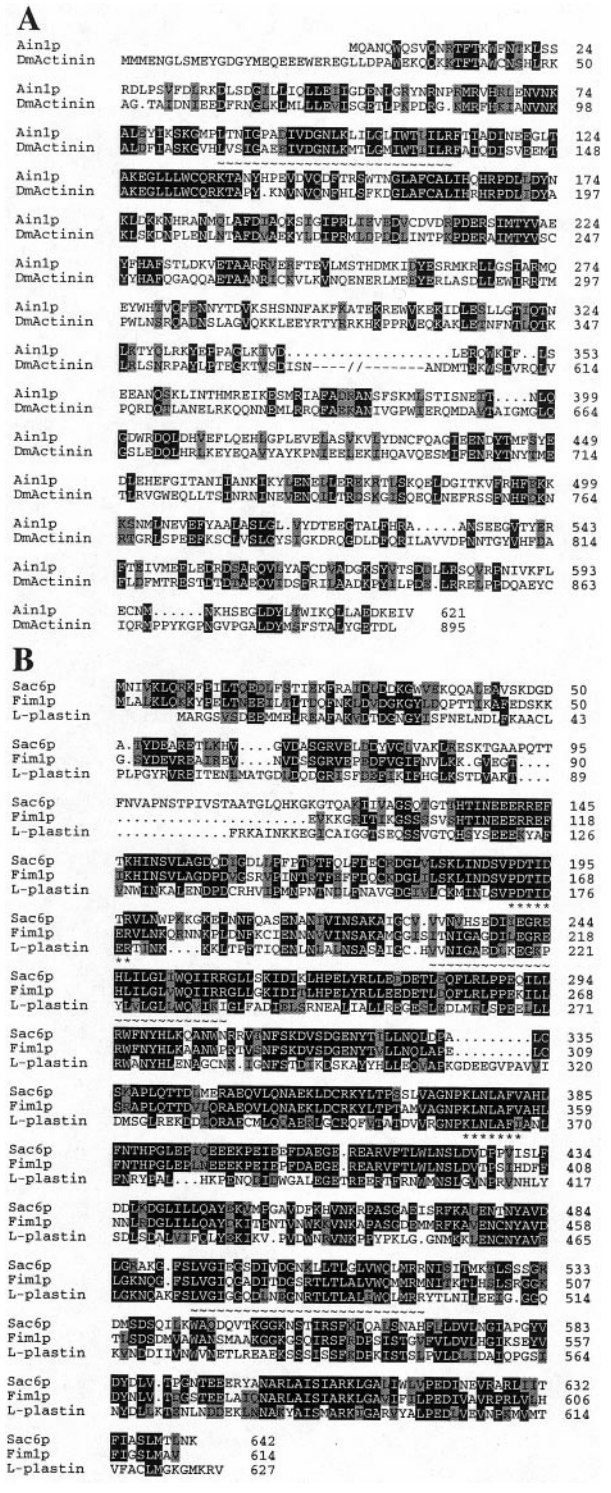

Figure 2. Sequences of *S. pombe* Ain1p and Fim1p. (A) Alignment of Ain1p (GenBank/EMBL/DDBJ accession number Z97208) and *Drosophila* muscle α-actinin (DmActinin; accession number X51753). Proteins were aligned using the GCG GAP program with some modifications according to the results of a BLAST analysis (http://www.ncbi.nlm.nih.gov/BLAST/). Identical and similar (V/I/L, D/E, K/R, N/Q, S/T) amino acids are shaded in black and gray, respectively. Dots indicate gaps introduced to optimize the alignment; underscoring by ~ indicates the presumed actin-binding motif; and –//– indicates amino acids 370 to 599 of DmActinin, omitted here to optimize alignment of the NH_2- and COOH-terminal regions of the proteins (see text). (B) Alignment of Fim1p (GenBank/EMBL/DDBJ accession number AF053722), *S. cerevisiae* Sac6p (SWISS-PROT accession number P32599), and the human fimbrin L-plastin (SWISS-PROT accession number P13796). Proteins were aligned using the GCG PileUp program. Amino acids identical or similar (see above) to those in Fim1p are shaded in black and gray, respectively. Two putative actin-binding motifs are underscored with ~. The amino acids of Sac6p and L-plastin underscored with * were used to design the degenerate PCR primers that allowed the cloning of *fim1* (see MATERIALS AND METHODS).

with two modifications. One-third volume of 16% EM-grade paraformaldehyde solution (Electron Microscopy Sciences, Ft. Washington, PA), preincubated to the same temperature as the culture, was added to a growing culture in EMM or YES medium, and fixation was continued for 15 min at the growth temperature. After staining with rhodamine-phalloidin, the cell suspension was mixed with an equal volume of 10 μg/ml bisBenzimide (in 0.1 M Na Pipes, pH 6.9, 1 mM EGTA, 1 mM $MgSO_4$) to visualize DNA. For double staining of Fim1p-3HA and actin, immunofluorescence was carried out essentially as described above, except that cells were in suspension in a microfuge tube rather than affixed to a slide. The cells were then stained with rhodamine-phalloidin (as described above) just before mounting and observation.

To determine the effects of actin depolymerization on the localization of Ain1p and Fim1p, cells were grown in EMM medium at 25°C to 5×10^6 cells/ml, and then Latrunculin A (Lat-A; Molecular Probes) was added from a 20 mM stock solution in DMSO to a final concentration of 100 μM; a control culture received an equal volume of DMSO. Incubation was continued for 20 min at 25°C, and cells were double-stained with Calcofluor and bisBenzimide or fixed and stained with rhodamine-phalloidin or HA-specific antibodies (see above).

RESULTS

Identification of an α-Actinin Homologue and of a Fimbrin in S. pombe

The *S. pombe* genome project revealed an open reading frame (here designated *ain1*) on cosmid c15A10 of chromosome I that encodes an α-actinin-like protein (Ain1p). *ain1* contains two presumed introns (with consensus donor, splice-branch, and acceptor sequences) of 51 and 140 bp, and Ain1p is predicted to contain 621 amino acids. It is 32–35% identical to *Dictyostelium* α-actinin (Noegel *et al.*, 1987), *Drosophila* muscle α-actinin (Fyrberg *et al.*, 1990), and human nonmuscle α-actinin-1 (SWISS-PROT accession number P12814; Millake *et al.*, 1989) over its entire length and ~50% identical to these proteins over its NH_2-terminal 222 amino acids, which include a conserved actin-binding motif (Bresnick *et al.*, 1990) of 27 amino acids (Figure 2A). Amino acids 225–343 of Ain1p are 27% identical to the first spectrin-like repeat (amino acids 248–366) of *Drosophila* muscle α-actinin, and amino acids 344–450 of Ain1p are 21% identical to the fourth spectrin-like repeat (amino acids 603–715) of the *Drosophila* protein (Figure 2A). (These two regions of Ain1p are less similar to the second and third repeats of the *Drosophila* protein, which have thus been omitted from Figure 2A.) Thus, it seems that Ain1p has only two spectrin-like repeats, consistent with its shorter overall length compared with the

other known α-actinins. Amino acids 487–550 of Ain1p are 28% identical to the two EF-hand motifs (amino acids 752–821) of *Drosophila* muscle α-actinin, but this region of Ain1p does not appear likely to contain a functional Ca^{2+}-binding site (Strynadka and James, 1989). Ain1p and the *Drosophila* protein are also ~30% identical over their COOH-terminal ~70 amino acids. No other obvious motifs were found in Ain1p, except for one small region (amino acids 137–153) having 47% identity (65% similarity) to the phosphatidylinositol 4,5-bisphosphate-binding site in chicken muscle α-actinin (Fukami *et al.*, 1996).

The mild phenotype of *ain1* deletion cells (see below) suggested that Ain1p might overlap in function with another actin-binding protein. Although no obvious candidate had been identified by the genome project, the presence of a fimbrin (Sac6p) in *S. cerevisiae* (Adams *et al.*, 1991) suggested that *S. pombe* might also contain a fimbrin. Indeed, PCR using degenerate primers based on two regions conserved among known fimbrins yielded a product with strong similarity to other fimbrin genes (see MATERIALS AND METHODS). Use of this fragment to probe a genomic-DNA library yielded a plasmid containing a complete fimbrin coding sequence (here designated *fim1*) interrupted by two introns, as confirmed by the analysis of cDNA sequences (see MATERIALS AND METHODS). Sequences subsequently released by the genome project (cosmid c1778 on chromosome II) were identical within the *fim1* coding region.

The predicted Fim1p sequence of 614 amino acids is very similar (64, 49, and 42% identical, respectively, over the full lengths of the proteins) to those of *S. cerevisiae* Sac6p (Adams *et al.*, 1991), *Dictyostelium* fimbrin (Prassler *et al.*, 1997), and human L-plastin (Lin *et al.*, 1988, 1990) (Figure 2B). Like these related proteins, Fim1p has two apparent actin-binding motifs that are 41% identical to each other. The first of these (amino acids 205–231) is 56% identical to the putative actin-binding motif in Ain1p (Figure 2A), whereas the second (amino acids 467–493) is 41% identical to that in Ain1p. Like Sac6p (Adams *et al.*, 1991), Fim1p does not appear to have EF-hand-like motifs that would be functional for Ca^{2+} binding (Strynadka and James, 1989).

Actin-dependent Localization of Ain1p to the Medial Ring and of Fim1p to the Medial Ring and Actin Patches

To localize Ain1p, we tagged the chromosomal *ain1* locus with GFP-encoding sequences both at its 3′ end (*ain1*$^+$*-GFP*, under the *ain1* promoter) and at its 5′ end (*41nmt1-GFP-ain1*$^+$ and *81nmt1-GFP-ain1*$^+$, regulated by the attenuated *nmt1* promoters). When cells expressing Ain1p-GFP were examined, no signal was detected in interphase cells (Figure 3A, cell 1). In anaphase cells, Ain1p formed a ring in the middle of the cell (Figure 3A, cells 2–5). The time of appearance and localization of this ring were similar to those of other components of the medial ring (Gould and Simanis, 1997). The Ain1p ring then gradually contracted to a dot and disappeared as the septum formed; Ain1p was always at the leading edge of the centripetally growing septum (Figure 3A, cells 6–10). At no stage was Ain1p-GFP observed in the actin patches or cables. However, it seemed possible that Ain1p was actually present in these structures but that the Ain1p-GFP signals were too weak to detect. To test this possibility, we also examined the strains expressing GFP-Ain1p from the attenuated *nmt1* promoters. When grown under repressing conditions, *41nmt1-GFP-ain1*$^+$ cells had a stronger GFP signal than did *ain1*$^+$*-GFP* cells, but the Ain1p localization pattern was the same. When grown under inducing conditions, *81nmt1-GFP-ain1*$^+$ cells had an even stronger GFP signal. This signal was again localized primarily to the medial ring. However, when the cells were grown for ≥20 h under inducing conditions, Ain1p was also observed as a dot near the nucleus in some interphase cells (our unpublished results). Double staining to determine whether this dot corresponded to the spindle pole body was not possible because the GFP signal did not survive preparation of cells for immunofluorescence. Attempts to gain more information by tagging Ain1p with 3HA were unsuccessful (our unpublished results): either no signal was observed by immunofluorescence (COOH-terminal tag) or localization was observed only to the medial ring (NH_2-terminal tag under control of the *nmt1* promoter). In summary, the localization of Ain1p suggested that it might be involved mainly in cytokinesis and/or septum formation.

To localize Fim1p, we tagged the chromosomal *fim1* locus at its 3′ end with sequences encoding 3HA or GFP, so that the tagged proteins would be expressed from the *fim1* promoter. When cells expressing Fim1p-3HA were examined by immunofluorescence, protein localization was detected throughout the cell cycle. In interphase cells and cells early in mitosis, Fim1p-3HA was found in patches that were concentrated at one (smaller cells; Figure 3B, cell 1) or both (larger cells; Figure 3B, cells 2–5) ends of the cells. Double staining revealed that Fim1p and actin were colocalized in these patches (Figure 3C). In early anaphase, Fim1p-3HA was still detectable in patches near the cell poles, but a medial ring-like structure also appeared (Figure 3B, cells 6–8). Later in anaphase, the medial ring became more prominent, and few patches (typically concentrated near the medial ring) were observed (Figure 3B, cells 9 and 10). Thus, the localization of Fim1p-3HA closely paralleled that of actin (Marks and Hyams, 1985; see also Figures 4B and 6), except that Fim1p-3HA was not observed in association with actin cables and that the Fim1p ring did not appear to contract at the time of septum formation (Figure 3B, cells 9 and 10; see DISCUSSION). Examination of cells expressing Fim1p-GFP revealed patches at the cell tips and division site like those seen in the cells expressing Fim1p-3HA (except that the patches at the division site were more pronounced during septum formation). However, the medial-ring-like structure was not clearly or consistently visualized with Fim1p-GFP, perhaps because it was obscured by the prominent and rapidly moving (our unpublished results) patches or because Fim1p-GFP was not fully normal in function (see MATERIALS AND METHODS).

To determine whether the localizations of Ain1p and Fim1p depend on F-actin, we treated *ain1*$^+$*-GFP* and *fim1*$^+$*-GFP* cells with the inhibitor Lat-A, which specifically and efficiently disrupts actin filaments in *S. pombe* (Ayscough *et al.*, 1997; Bähler and Pringle, 1998; Figure 4, A and B). Although treatment with DMSO alone had no obvious effect on the localization of Ain1p-GFP or Fim1p-GFP, localization of Ain1p-GFP (Figure 4, C and D) and of

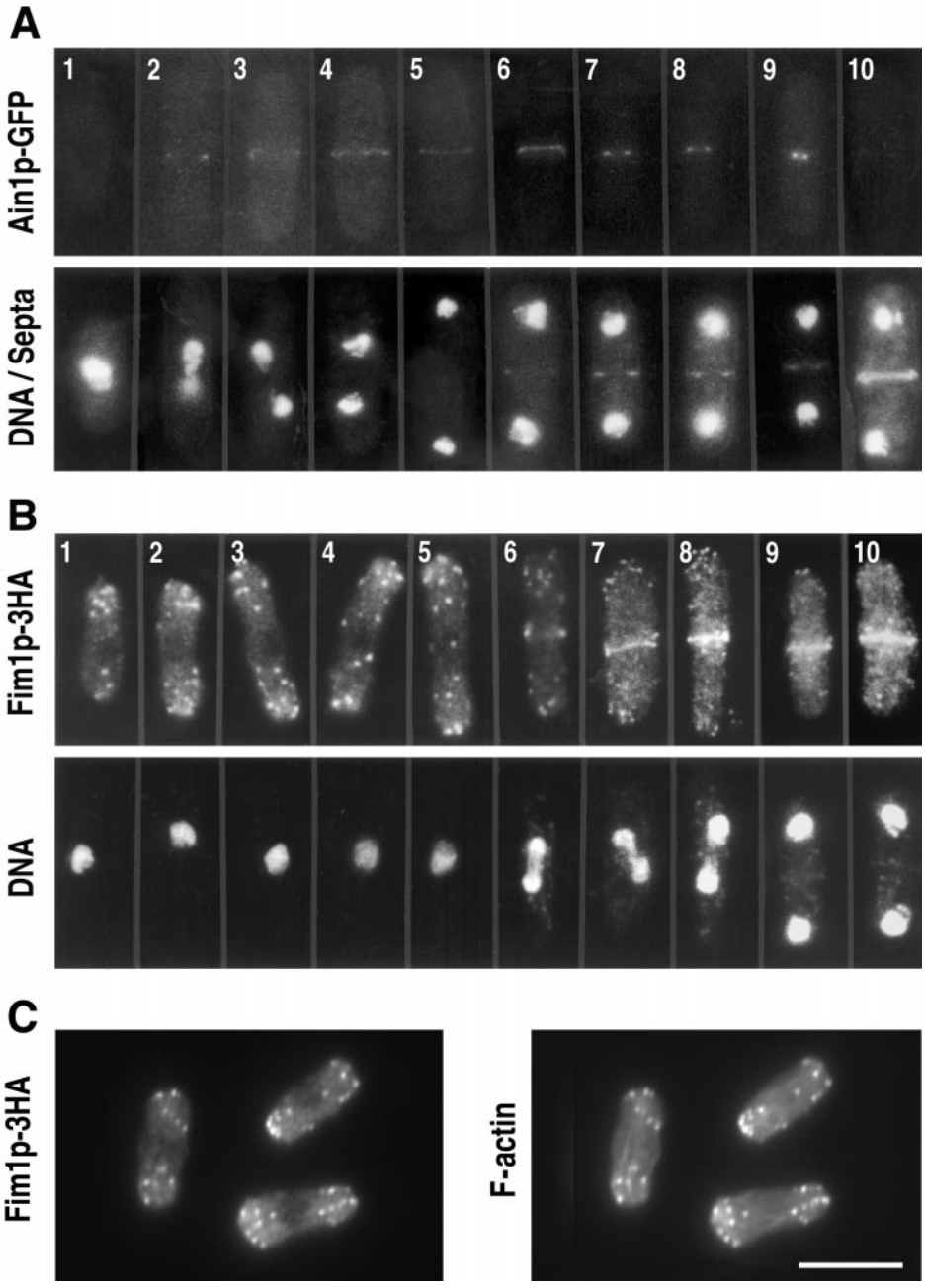

Figure 3. Localization of Ain1p and Fim1p during the cell cycle. In A and B, upper and lower panels show the same cells, and individual cells are numbered for reference in the text; in C, the two panels show the same cells. (A) Localization of Ain1p to the medial ring. Cells expressing Ain1p-GFP (strain JW46) were grown in EMM medium at 25°C and stained with Calcofluor and bisBenzimide to allow visualization of septa and DNA. (B and C) Localization of Fim1p to actin patches and the medial ring. Cells expressing Fim1p-3HA (strain JW106) were grown in EMM at 30°C, fixed, and double-stained either with HA-specific antibody and bisBenzimide (B) or with HA-specific antibody and rhodamine-phalloidin (C). Bar, 10 μm.

Fim1p-GFP (Figure 4, E and F) was completely lost in cells treated for 20 min with Lat-A in DMSO. Similar results (including a loss of medial-ring localization) were obtained with cells expressing Fim1p-3HA (strain JW106). Thus, the localizations of both Ain1p and Fim1p appear to depend on F-actin.

Involvement of Ain1p in Cell Division

To investigate the function of Ain1p, we constructed a strain (JW45) carrying a complete deletion of the *ain1* coding sequences (*ain1-Δ1*). The *ain1-Δ1* cells grew at a normal rate on YES or EMM medium at temperatures from 18 to 36°C and

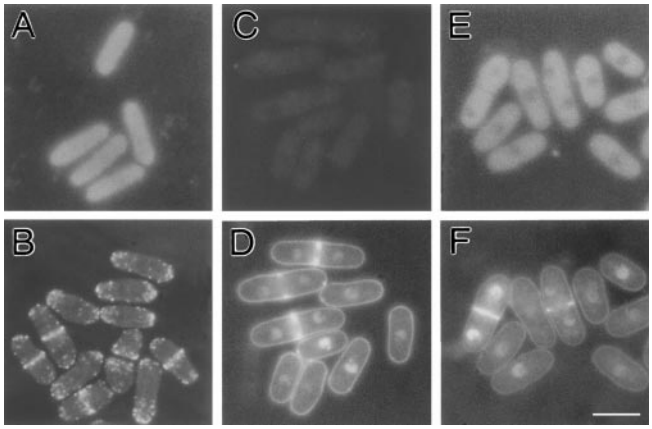

Figure 4. Actin dependence of Ain1p and Fim1p localization. Cells expressing Ain1p-GFP (strain JW46; A-D) or Fim1p-GFP (strain JW109; E and F) were treated with 100 μM Lat-A (added from a stock solution in DMSO; see MATERIALS AND METHODS) (A and C–F) or an equal volume of DMSO alone (B) at 25°C for 20 min, and then stained for actin (A and B) or examined for the GFP-fusion proteins (C and E) after staining with Calcofluor and bisBenzimide to allow visualization of septa and DNA in the same cells (D and F). Bar, 10 μm.

displayed no obvious defects in overall cell morphology or in actin organization (Figure 5A; and our unpublished results). However, under the stress conditions of low temperature and high salt (EMM + 1 M KCl medium at 18°C), *ain1-Δ1* cells grew much more slowly than wild type; moreover, although wild-type cells maintained a normal morphology under these conditions (Figure 5B), *ain1-Δ1* cells displayed pronounced abnormalities in cytokinesis and septation. In particular, some cells completed mitosis without forming septa or showing other indications of cytokinesis, some cells formed partial septa, some cells had double or triple septa, and some cells formed misplaced septa (Figure 5C). As expected for a defect affecting cytokinesis and septation but not other aspects of cell cycle progression, cells

Table 2. Accumulation of multinucleate cells during growth of an *ain1* deletion strain under stress conditions[a]

Strain	Time (h)	% of Cells with 1 nucleus	2 nuclei	3 or 4 nuclei	6 or 8 nuclei
wild type	60	77	23	0	0
ain1-Δ1	0	77	23	0	0
	20	72	28	<0.5	0
	40	4	87	9	<0.5
	60	13	45	35	7

[a]Cells of wild-type strain 972 and *ain1-Δ1* strain JW45 were fixed and stained with bisBenzimide at various times after shifting exponentially growing cells from YES medium at 30°C to EMM + 1 M KCl medium at 18°C. At least 300 cells were scored for each time point. Note that some *ain1-Δ1* cells appeared to die and lyse with 2-4 nuclei, and death and lysis were extensive among cells with eight nuclei.

with multiple nuclei accumulated in the *ain1-Δ1* strain (but not in the wild-type strain) during growth under the stress conditions (Table 2).

The abnormalities in cytokinesis and septation in the *ain1* deletion cells under stress conditions might result from abnormalities in actin organization. Indeed, although wild-type cells grown under the stress conditions displayed normal actin organization (Figure 6A, left panels), and *ain1-Δ1* interphase cells displayed a seemingly normal organization of actin patches (Figure 6A, right panels, cell 1), the *ain1-Δ1* cells did not develop normal medial-ring structures. Instead, early in mitosis, some cells formed aberrant, thin, cable-like structures in the cell middle when most of the actin patches were still at the cell tips (Figure 6A, right panels, cell 2; the cable-like structures were more apparent under the microscope than they are in the printed micrograph). In anaphase cells, the majority of the actin patches accumulated in a broad region around the cell middle (Figure 6A, right panels, cells 3 and 4), but distinct actin rings were rarely seen. In

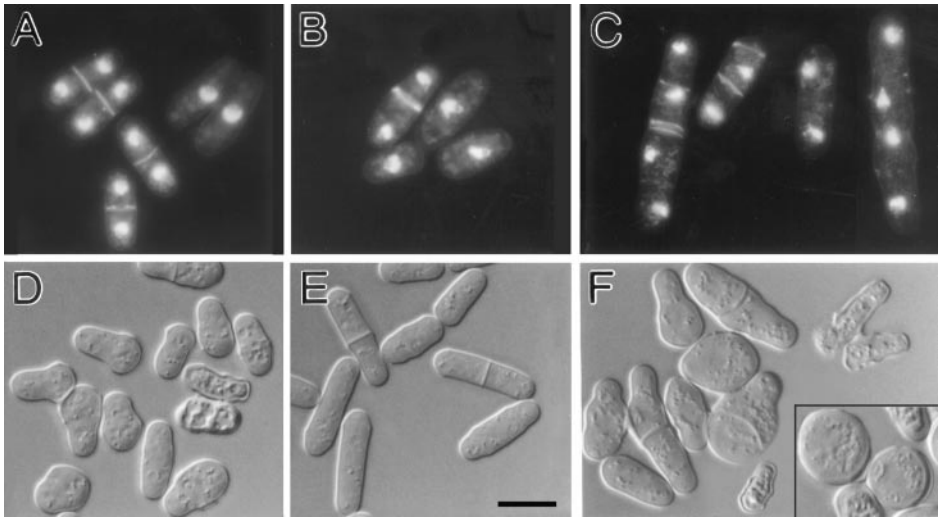

Figure 5. Morphological abnormalities of *ain1* deletion and *fim1* deletion cells. (A–C) Cells were double-stained with Calcofluor and bisBenzimide to visualize septa and DNA. (D–F) Cells were observed directly in culture medium by DIC microscopy. (A) *ain1-Δ1* cells (strain JW45) grown in EMM medium at 25°C. (B and C) Wild-type strain 972 (B) and strain JW45 (C) grown in EMM + 1 M KCl medium at 18°C for 40 h. (D) *fim1-Δ1* cells (strain JW142) grown in EMM at 25°C. (E and F) Strains 972 (E) and JW142 (F) grown for 5 h (20 h for the cells in the inset) after a shift from 25 to 36°C in EMM. Bar, 10 μm.

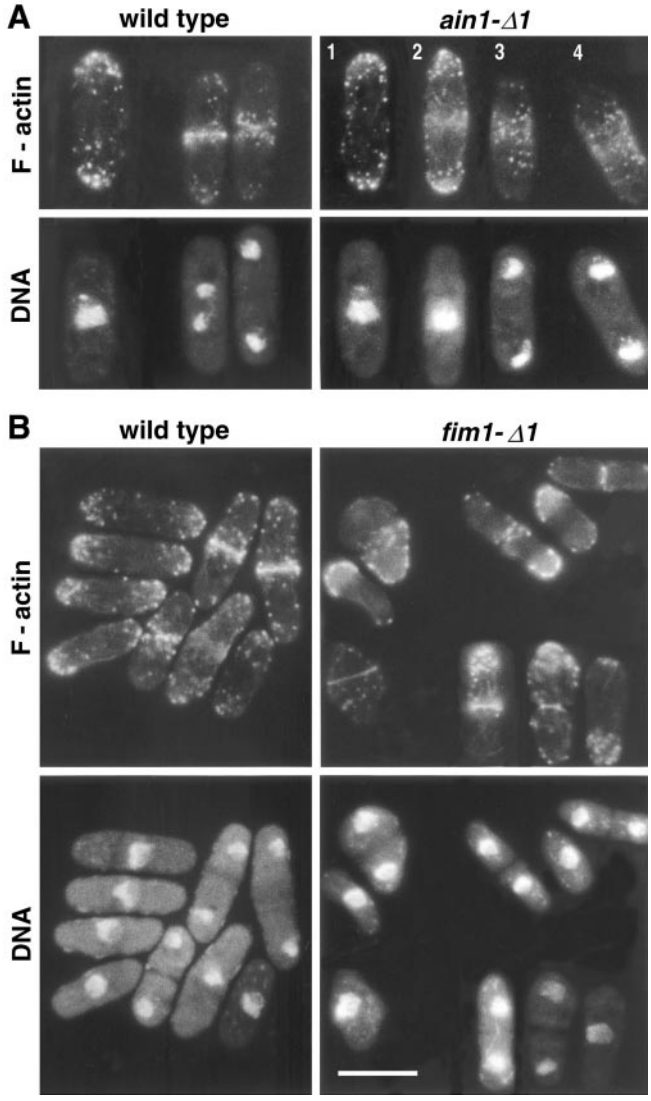

Figure 6. Abnormal actin organization in *ain1* deletion and *fim1* deletion cells. (A) Failure of actin-ring formation in *ain1-Δ1* cells under stress conditions. Strains 972 (left panels) and JW45 (right panels) growing in YES medium at 30°C were shifted to EMM + 1 M KCl medium at 18°C for 20 h, fixed, and double-stained with rhodamine-phalloidin (upper panels) and bisBenzimide (lower panels). (B) Mislocalization and disorganization of actin patches in *fim1-Δ1* cells. Strains 972 (left panels) and JW142 (right panels) growing in EMM medium at 25°C were shifted to 36°C for 5 h, fixed, and double-stained with rhodamine-phalloidin (upper panels) and bisBenzimide (lower panels). Bar, 10 μm.

~1% of anaphase cells, very thin ring-like structures that were difficult to photograph were seen at the cell middles. Thus, Ain1p appears to be involved in formation of the actin ring, at least under stress conditions.

A role for Ain1p in actin-ring formation, cytokinesis, and septation is also supported by the results of overexpression studies. To overexpress Ain1p, the promoter of the chromosomal *ain1* locus was replaced by the high-expression *3nmt1* promoter. When *3nmt1-ain1*$^+$ cells (strain JW49) were grown under repressing conditions, most cells looked normal, although ~5% had abnormal or double septa. After a shift to inducing conditions, cells with two or more nuclei accumulated in the population (Figure 7A, left panels); by 19 h of induction, ~60% of cells had two or more nuclei. Although most cells still formed septa, the septa were usually misoriented and/or disorganized, and some cells had double septa (Figure 7A, left panels). The Ain1p-overexpressing cells did not have other obvious morphological defects, which suggested that actin organization might be normal except for defects in actin-ring assembly. Indeed, rhodamine-phalloidin staining revealed an apparently normal organization and localization of actin patches in interphase cells (Figure 7B, left panels, arrowhead). In contrast, although most anaphase cells displayed actin-ring structures, these were generally misplaced and/or disorganized in ways that paralleled the abnormalities in septum organization (Figure 7B, left panels).

Additional evidence for a role of Ain1p in actin-ring organization was obtained by analyzing genetic interactions between *ain1-Δ1* and other mutations known to affect medial-ring positioning and/or organization. *ain1-Δ1* showed strong synthetic growth and cytokinesis defects with *act1-48* (actin), *myo2-E1* (myosin II), *cdc4-8* (myosin light chain-like protein), and *cdc3-6* (profilin), and weaker synthetic defects with *cdc8-110* (tropomyosin), *rng2-D5* (IQGAP), *cdc12-112* (a formin), *mid1-ΔF*, and *pom1-Δ1* (Table 3; and our unpublished results). In contrast, no genetic interactions were detected between *ain1-Δ1* and mutations affecting the regulation of septation (*cdc14-118* and *cdc16-116*), actin cortical-patch function (*arp3-c1*), or microtubule function (*nda3-KM311*) (see Table 1 for references), supporting the hypothesis that the function of Ain1p may be restricted to medial-ring assembly and positioning.

Involvement of Fim1p in Cell Polarization and Perhaps in Cell Division

To investigate the function of Fim1p, we constructed a strain (JW142) carrying a complete deletion of the *fim1* coding sequences (*fim1-Δ1*). Strain JW142 could grow on either YES or EMM medium at temperatures from 18 to 36°C, but it displayed a growth defect whose severity depended on the conditions. It grew at a rate similar to that of wild type in YES medium at 25°C but grew more slowly at higher temperatures and/or in EMM medium. On EMM at 36°C, it formed tiny colonies that were red when the plates contained phloxin, suggesting that many of the cells were dead, and it was unable to form colonies on EMM + 1 M KCl at temperatures from 18 to 36°C. The *fim1-Δ1* cells also displayed pronounced morphological defects in EMM medium; even at 25°C, ~30% of the cells (n = 492) were rounder than normal (Figure 5D), and 5% of the cells appeared dead (shrunken and phloxin red; some cells were clearly lysed). These defects were more pronounced at 36°C: although wild-type cells looked normal under these conditions (Figure 5E), by 5 h after a shift of *fim1-Δ1* cells from 25 to 36°C, ~16% of the cells (n = 488) appeared dead (among which about half were clearly lysed), and ~18% of the cells were clearly rounder than normal (Figure 5F). By 10 h at 36°C, ~21% of the *fim1-Δ1* cells (n = 419) appeared dead, and ~30% were rounder than normal. Beginning at ~10 h, and more frequently at later times, cells could be found that had

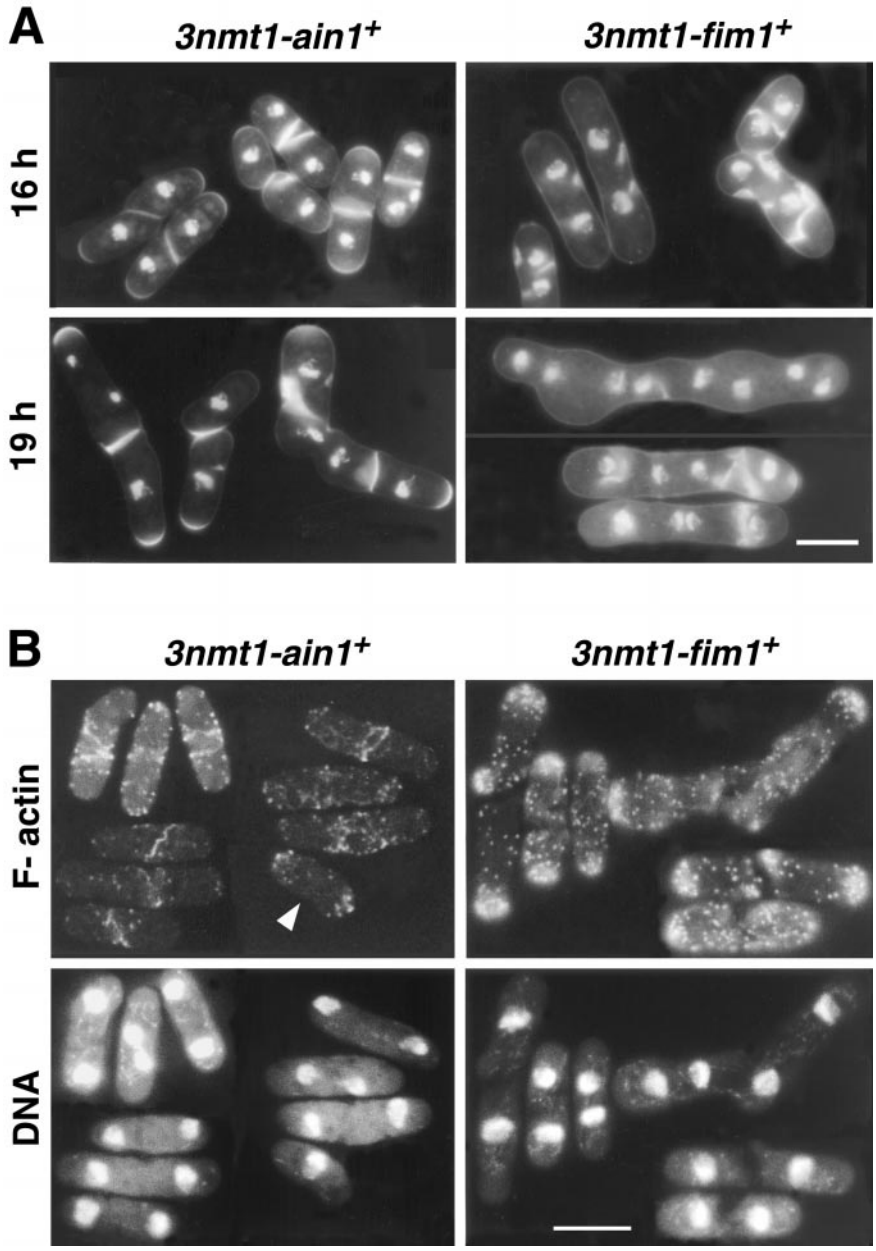

Figure 7. Defects in cytokinesis, septation, and actin organization resulting from overexpression of Ain1p or Fim1p. Cells in which the expression of Ain1p or Fim1p was under the control of the *3nmt1* promoter were grown under repressing conditions and then shifted to inducing conditions (see MATERIALS AND METHODS) at 30°C. (A) Cells of strains JW49 (left panels) and JW110 (right panels) were double-stained with Calcofluor and bisBenzimide at 16 h (upper panels) or 19 h (lower panels). (B) Cells of strains JW49 (left panels) and JW110 (right panels) were fixed and double-stained with rhodamine-phalloidin (upper panels) and bisBenzimide (lower panels) at 16 h. The arrowhead indicates an interphase cell (see text). Bars, 10 μm.

apparently lost polarity completely and were perfectly round (Figure 5F, inset). At either 25 or 36°C, the *fim1-Δ1* strain displayed a modest increase in the number of cells with two nuclei (~45% compared with the ~28% characteristic of wild type), but only ~1% of the cells had more than two nuclei. These data suggest either that cell division was generally completed (although possibly after some delay) even in the morphologically aberrant cells and/or that the nuclear cycle was also delayed (perhaps by a checkpoint function). *fim1-Δ1* cells plated on EMM + 1 M KCl medium at 18, 25, or 36°C also did not display any obvious defect in cytokinesis or septation.

It seemed likely that the partial loss of growth polarization in *fim1* deletion cells reflected defects in the organization of the actin cytoskeleton. Indeed, although wild-type cells showed normal actin distribution in EMM medium at 36°C (Figure 6B, left panels), *fim1-Δ1* cells did not display normal actin patches under these conditions. Instead, the patches appeared to be disorganized and mislocalized: they were not usually distinct, they sometimes appeared to fuse to form a cap-like structure at the cell end, and they also covered a larger area than just the cell tips (Figure 6B, right panels). The actin patches in the perfectly round cells were uniformly distributed in the cell cortex, indicating that the cells had completely lost polarity. Consistent with the absence of an obvious cytokinesis defect, actin rings appeared to form normally (Figure 6B, right panels). However, the actin patches did not relocalize efficiently to the cell middle;

Table 3. Genetic interactions of *ain1-Δ1* with other mutations affecting medial-ring positioning and/or organization

Mutant	Growth at the indicated temperature[a]		
	25°C	30°C	32°C
ain1-Δ1	++++	++++	++++
act1-48	+++	+++	+++
ain1-Δ1 act1-48	−	+	+
myo2-E1	+++	+++	+++
ain1-Δ1 myo2-E1	+	−	−
cdc3-6	+++	+++	++
ain1-Δ1 cdc3-6	+	−	−
rng2-D5	++++	+++	++
ain1-Δ1 rng2-D5	+++	++	−
mid1-ΔF	+++	+++	+++
ain1-Δ1 mid1-ΔF	++	++	++

[a] Double mutants were constructed by crossing appropriate strains (Table 1), dissecting tetrads, and incubating at 25 or 32°C as needed to recover viable double-mutant clones. To evaluate growth at different temperatures, cells were diluted to yield single colonies on YES medium containing phloxin B (see MATERIALS AND METHODS) and incubated at the temperatures indicated. (++++) Colony formation similar to wild type and nearly all cells healthy (phloxin-pink); (+++) medium-size colonies with some dead cells (phloxin-red); (++) small colonies with substantial numbers of dead cells (phloxin-red); (+) very slow growth, tiny colonies with large numbers of dead cells (phloxin-dark red); (−) no colony formation.

thus, when the actin ring had formed and begun to contract, considerable F-actin remained at the cell tip(s) (Figure 6B, right panels), which was never observed in wild-type cells. It was also striking that some cells at this stage appeared to have the actin patches concentrated at one pole of the cell; in contrast, wild-type cells always have patches concentrated at both poles before medial-ring formation. The *fim1-Δ1* cells still had actin cables, but these were difficult to photograph and thus are difficult to see in the printed micrographs.

The data described above suggested that Fim1p might be involved in polarization of cell growth and/or actin cortical-patch function, a hypothesis that was further supported by genetic evidence. In particular, *fim1-Δ1* was synthetically lethal with the cold-sensitive *arp3-c1* mutation: no double mutant was recovered on YES medium at either 30 or 32°C (conditions permissive for both single mutants) from 17 tetrads dissected. The 15 predicted double-mutant segregants germinated and then died as 1–30 small, round cells; no elongated cells were found. Thus, it appeared that the double mutant was defective in polarized growth but not in cytokinesis.

However, a possible role for Fim1p in cytokinesis and/or septation was suggested by overexpression studies. To overexpress Fim1p, the promoter of the chromosomal *fim1* locus was replaced by the *3nmt1* promoter. *3nmt1-fim1*$^+$ cells (strain JW110) were indistinguishable from wild-type cells under repressing conditions, but a pronounced defect in cytokinesis and septation was observed after a shift to inducing conditions. The number of cells with two or more nuclei increased dramatically (Figure 7A, right panels; by 19 h, 44% of the cells had two nuclei, 43% had four, and 8% had eight), and septum formation was grossly defective (Figure 7A). Some cells did not appear to deposit any septal material, others deposited small amounts of such material at normal or abnormal locations, and still others did form aberrant septa, but no cells formed normal-looking septa. In addition, these cells had severe defects in the organization of F-actin. No actin rings or concentrations of actin patches in the cell middles were detectable, although many patches were not at the cell tips (Figure 7B, right panels). Most of the actin patches at the cell tips were more brightly stained than those in wild-type cells (grown and stained at the same time), but their organization otherwise appeared normal (Figure 7B; cf. the wild-type cells in Figures 4B and 6). The actin cables also appeared normal but were difficult to photograph.

Synthetic Lethality and Cell Division Defect of an ain1 fim1 *Double Mutant*

To ask whether Ain1p and Fim1p overlap in function, *ain1-Δ1* (JW45) and *fim1-Δ1* (JW142) strains were crossed, and tetrads were dissected onto YES plates at 25°C. From 36 tetrads, all 35 predicted double mutants were inviable; 34 arrested as a single, highly elongated cell, and one arrested after two cell divisions. Thus, *ain1-Δ1* and *fim1-Δ1* were synthetically lethal under conditions in which both single mutants resembled wild type (see above).

The elongated morphology of the double-mutant cells suggested that they might be defective in cytokinesis and/or septation. To explore this possibility, an *ain1-Δ1* strain (JW53) was crossed to a strain (JW111) with the wild type *fim1*$^+$ coding sequence under control of the attenuated *41nmt1* promoter. Strain JW111 itself resembled wild type under both inducing and repressing conditions. However, no *ain1-Δ1 41nmt1-fim1*$^+$ double mutant was recovered on YES plates (repressing conditions) from 19 tetrads dissected; the 22 predicted double mutants arrested as one to several hundred highly elongated cells with no septa or with aberrant septa. However, *ain1-Δ1 41nmt1-fim1*$^+$ double mutants were recovered by germinating spores on EMM (inducing conditions). The double mutants were indistinguishable from wild type under inducing conditions (Figure 8A) but had severe defects in cytokinesis and septation under repressing conditions and could form only tiny colonies at 25°C and no visible colonies at 36°C. The cell division defect became evident within 12 h after a shift to repressing conditions; by 16 h, 98% of the cells (n = 346) had two or four nuclei, while some cells had no septa and other cells had partial or misplaced septa (Figure 8, B and C). A few cells did have seemingly complete septa (which might have formed before Fim1p was depleted) but were delayed or defective in cell separation (Figure 8, B and C). By 24 h under repressing conditions, most cells had accumulated four or eight nuclei and begun to lyse. The defects in cytokinesis and septation were associated with severe defects in medial-ring assembly and/or positioning and in the concentration of actin patches at presumptive septation sites (Figure 8, D and E). The cells also displayed misplaced and aberrant cable-like structures (Figure 8, D and E) that were distinct from the weakly stained actin cables normally seen in the cytoplasm of wild-type cells. Thus, it appears that Ain1p and Fim1p play overlapping roles in the organization of actin for cytokinesis and septation.

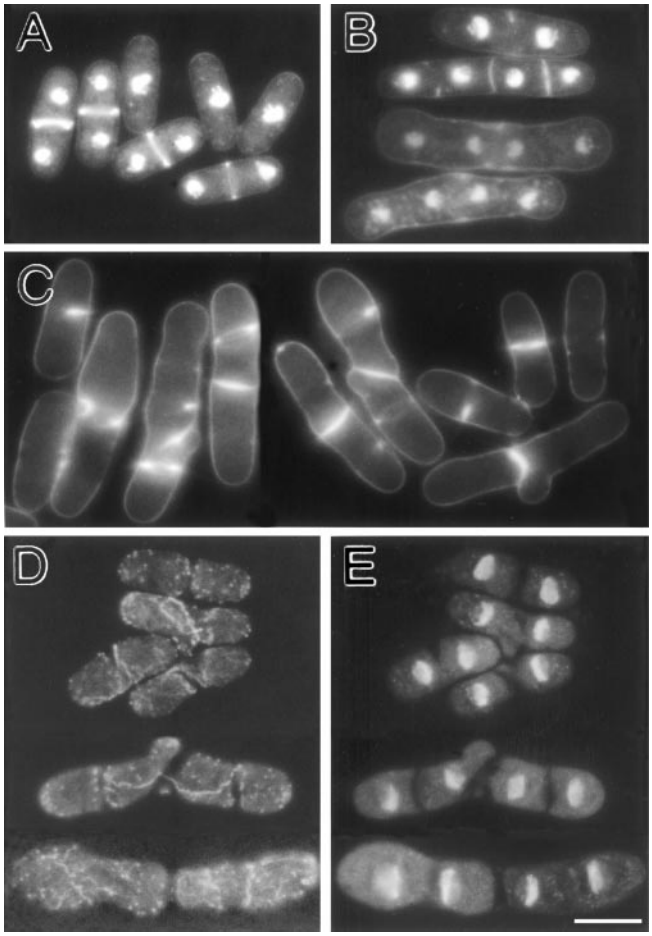

Figure 8. Cell division defect of an *ain1 fim1* double mutant. *ain1-Δ1 41nmt1-fim1*$^+$ cells (strain JW164) growing in EMM medium without thiamine (inducing conditions) at 25°C (A) or 16 h after a shift to YES medium (repressing conditions, leading to depletion of Fim1p) at 25°C (B–E) were double-stained for septa and DNA without fixation (A and B), stained for septa alone without fixation (C), or double-stained for F-actin (D) and DNA (E) after fixation (see MATERIALS AND METHODS). Bar, 10 μm.

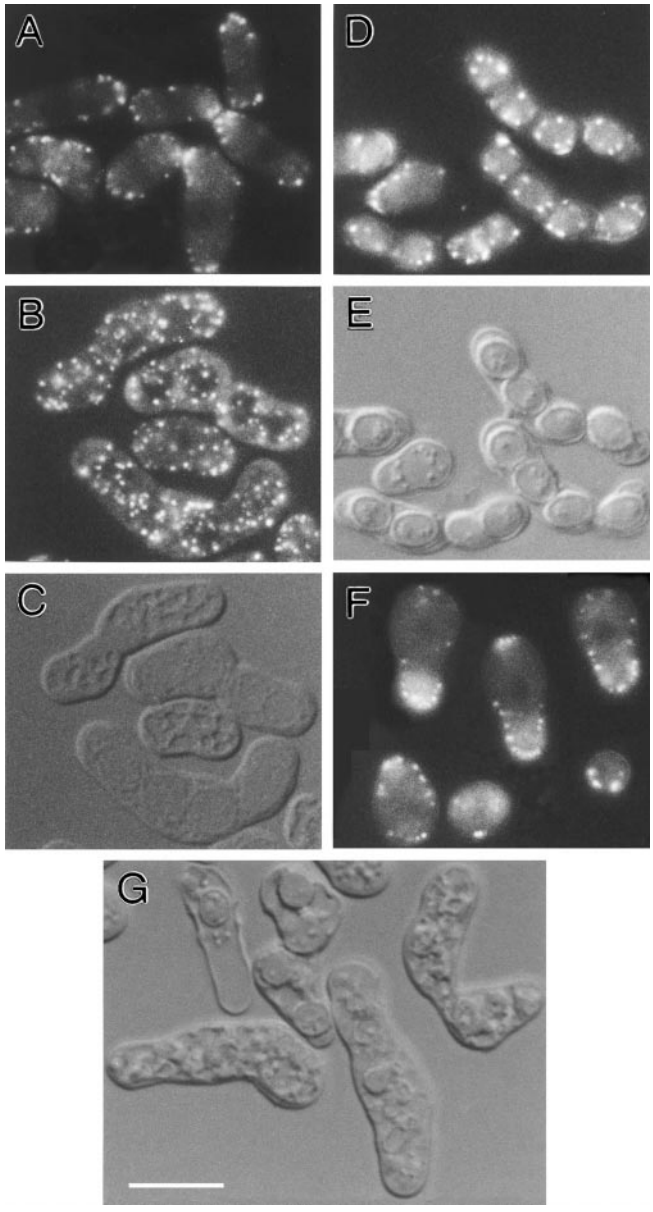

Figure 9. (A–F) Localization of Fim1p-GFP during mating (A), sporulation (B and D), and spore germination (F). (C and E) DIC images of the cells shown in B and D, respectively. *fim1*$^+$*-GFP* strains JW109 and JW117 were crossed on an SPA plate at 25°C, and samples taken after 12 h (A), 24 h (B and C), and 50 h (D and E) were examined after resuspension in liquid SPA medium. After 60 h, the mature asci were digested with Glusulase (NEN, Boston, MA) to release spores, which were then incubated in liquid EMM medium at 25°C and examined after 12 h (F). (G) Defective sporulation in *fim1* deletion cells. *fim1-Δ1* strains JW144 and JW142 were crossed on an SPA plate at 25°C and examined by DIC after 50 h. Bar, 10 μm.

Involvement of Fim1p, but Apparently Not of Ain1p, in the Sexual Cycle

To investigate the possible functions of Ain1p and Fim1p during mating, sporulation, and spore germination, we examined the localizations of these proteins during these processes. When *ain1*$^+$*-GFP* strains of opposite mating type (strains JW46 and JW52) were mated, no localized signal was detected at any stage of the sexual cycle. As expected from this result, mating *ain1-Δ1* strains of opposite mating type (strains JW45 and JW53) resulted in spore formation as efficient as that in wild type.

In contrast, Fim1p-GFP was detectable at all stages in patches resembling those seen in vegetative cells. During mating, most of these patches were localized to the extended tips of the conjugating cells (Figure 9A). Later, when most asci had begun to form spores, the Fim1p-GFP patches localized predominantly to the cortices of the developing spores (Figure 9, B and C), and this localization was maintained in mature asci (Figure 9, D and E). Before germination, the Fim1p-GFP patches did not appear polarized in the spores, but upon germination, the Fim1p-GFP patches were concentrated in the growing tips (Figure 9F). Throughout

the sexual cycle, the localization of Fim1p was very similar to that of actin (Petersen *et al.*, 1998). These data suggest that Fim1p might be involved both in growth polarization during mating and spore germination and in the formation of the spore plasma membrane and/or spore wall. Support for these possibilities was provided by the defective mating and sporulation of *fim1* deletion strains. Fifty hours after crossing two *fim1*-Δ*1* strains, only ~16% of the cells had become asci (compared with ~51% in wild type), apparently reflecting at least in part a defect in mating. Moreover, <20% of the asci (n = 300) had four spores, while the others had zero to three spores (Figure 9G), and longer incubation did not change these numbers appreciably. The defect appeared to be in spore formation rather than in meiosis, because DNA staining revealed that most asci contained four nuclei. In contrast, >97% of the asci from a cross of wild-type strains 972 and 975 had four spores under the same conditions.

DISCUSSION

Evolution and Functional Relationships of Actin-bundling Proteins

α-Actinins and fimbrins are members of a family of actin cross-linking proteins that share very similar actin-binding domains; this family also includes spectrin, dystrophin, ABP-120, filamin, and cortexillin (reviewed by Matsudaira, 1994a; Faix *et al.*, 1996; Furukawa and Fechheimer, 1997; Bartles, 2000). As shown in this study, there are at least two members of this family in *S. pombe.* Fim1p appears to be a typical fimbrin, having strong similarity to other fimbrins throughout its sequence. In contrast, Ain1p is less similar in sequence to other known α-actinins and is also considerably shorter, having just two spectrin-like repeats instead of the usual four. Because sequence alignments and phylogenetic trees suggest that spectrins evolved from α-actinin by duplications of the spectrin-like repeats (Pascual *et al.*, 1997), it seems plausible that other modern α-actinins evolved from an ancestral Ain1p-like protein by duplication of its two repeats.

The relatively short length of Ain1p may have important functional implications. The observation that α-actinins and fimbrins bind to the same region of actin (Matsudaira, 1994b) suggests that they may have related but complementary functions. Indeed, it appears that these two proteins typically mediate the formation of distinct types of actin filament bundles. In particular, fimbrins, with their two closely spaced actin-binding domains, appear to form very tightly packed bundles, whereas α-actinins, whose actin-binding domains are at the opposite ends of the long homodimers, appear to form looser bundles (Meyer and Aebi, 1990; Drenckhahn *et al.*, 1991; Alberts *et al.*, 1994; Höfer and Drenckhahn, 1996; Djinovic-Carugo *et al.*, 1999; Bartles, 2000). In contrast to the bundles formed by typical α-actinins, those formed by the putative Ain1p homodimers would presumably be more tightly packed and hence more similar to the bundles formed by fimbrins. This similarity may help to explain the apparent partial overlap in function between Ain1p and Fim1p during cytokinesis (see also below). Such functional overlap between α-actinin and fimbrin does not appear to be typical: although these two proteins may both be involved in connecting actin filaments to the plasma membrane at sites of cell adhesions in some types of cells (Matsudaira, 1994a), we are not aware of other evidence for functional overlap between these proteins in cell types other than *S. pombe.*

In this regard, it is also interesting that *S. cerevisiae* contains no α-actinin–like protein and has the fimbrin Sac6p as its only member of this protein family (Ayscough, 1998). Because the homology between Ain1p and other α-actinins suggests strongly that the common ancestor of the fungi, protozoa, slime molds, and animals possessed an α-actinin–like protein, this protein must have been lost during the evolution of *S. cerevisiae.* The contrast with *S. pombe* is particularly striking because the actin cytoskeletons of the two yeasts seem generally quite similar in organization and function (Marks and Hyams, 1985; Botstein *et al.*, 1997; Gould and Simanis, 1997; Bähler and Peter, 2000; Pruyne and Bretscher, 2000). However, one significant difference is in the relative importance of the actomyosin contractile ring during cytokinesis. Although myosin II and the contractile ring are essential for cytokinesis in *S. pombe* (Bezanilla *et al.*, 1997; Kitayama *et al.*, 1997; May *et al.*, 1997; Motegi *et al.*, 1997), they are not essential in *S. cerevisiae* (Bi *et al.*, 1998; Lippincott and Li, 1998). A possible explanation for this difference is that the primary role of the contractile ring is to guide septum deposition (Hales *et al.*, 1999; Vallen *et al.*, 2000) and that the need for such guidance is greater in forming the ~3-μm-diameter septum in *S. pombe* than in forming the ~1-μm-diameter septum in *S. cerevisiae.* In any case, it seems possible that an Ain1p-like protein was rendered dispensable in *S. cerevisiae* by the combination of functional redundancy with Sac6p and the nonessential role of the actomyosin ring in cytokinesis.

It is also important to note that although we found no evidence for a role of Ain1p other than in cytokinesis, Fim1p clearly also has a distinct role(s) in the organization of the actin cytoskeleton in interphase cells (see also below). However, this other Fim1p role is also nonessential. Although it remains possible that this nonessentiality reflects redundancy with an unidentified member of the α-actinin/fimbrin family, it seems more likely (with the *S. pombe* genome sequence ~90% complete) that it reflects overlap in function with another type(s) of actin-binding protein, as appears to be the case also for Sac6p in *S. cerevisiae* (Adams *et al.*, 1993). Partial overlap in function between α-actinin and the structurally unrelated 34-kDa actin-bundling protein has also been observed in *Dictyostelium* (Rivero *et al.*, 1999).

Roles of Ain1p and Fim1p in Cytokinesis

Several lines of evidence indicate that Ain1p functions specifically in the contractile medial ring during cytokinesis. First, Ain1p was detected exclusively in this structure. Second, *ain1* deletion cells display cell division defects under stress conditions, much as do cells lacking the nonessential myosin II Myp2p/Myo3p (Bezanilla *et al.*, 1997; Motegi *et al.*, 1997). Third, cells overexpressing Ain1p have defects in cell division. Fourth, the *ain1* deletion mutation shows negative genetic interactions with several other mutations affecting medial-ring formation and cytokinesis. In contrast, the putative role of Fim1p in cytokinesis is less obvious. In *fim1* deletion cells, actin patches do not relocalize normally from the cell tip(s) to the cell center at the time of division, and some cells are lysed. In at least some cases, the lysis appeared to have occurred just after cell separation (our un-

published results), suggesting that it may result from defective cell wall or plasma membrane deposition at the new cell end. Moreover, at least some cells are delayed in cell division, as reflected by an increase in cells with two nuclei. These findings suggest that Fim1p might be involved in the targeted delivery of cell surface materials during cell division, much like its probable role during the polarized growth of interphase cells (see below). In addition, the localization of Fim1p to the medial ring and the cytokinesis defect of cells overexpressing Fim1p suggest that Fim1p may also be directly involved in medial-ring formation and/or function. This suggestion is strongly supported by the synthetic-lethal cytokinesis defect of cells lacking both Ain1p and Fim1p; this result also indicates that the roles of these two proteins in the medial ring are at least partly redundant.

What might be the role(s) of Ain1p and Fim1p in the medial ring? Medial-ring precursors start to accumulate at the cell center during the early stages of mitosis but only coalesce into a distinct ring during anaphase (Arai *et al.*, 1998; Bähler *et al.*, 1998a). Ain1p, Fim1p, and other actin-binding proteins such as Rng2p (Eng *et al.*, 1998) may be involved in organizing the medial-ring precursors into a functional contractile ring (for review, see Bähler and Peter, 2000). Consistent with this hypothesis, the ring localization of both Ain1p and Fim1p depends on actin, and actin forms only aberrant cables and localizes to a broad region in *ain1 fim1* double-mutant cells or in *ain1* single-mutant cells under stress conditions. In the latter case, at least, the actin structures resemble those seen during the early transient stage of medial-ring formation in wild-type cells. In some cases, pairs of actin cross-linking proteins appear to function sequentially in assembling a final structure (Tilney *et al.*, 1998; Bartles, 2000). However, Ain1p and Fim1p appear to assemble into the medial-ring structure at about the same time, consistent with the evidence for overlap in function.

In contrast, when the medial ring contracts, Ain1p stays at its leading edge while Fim1p appears to remain in an uncontracted ring. Although it is possible that the accumulation of Fim1p patches at the cell center obscures the detection of a contracting ring (as can happen when cells are stained for actin; see Balasubramanian *et al.*, 1997), it is also possible that actin filaments are bundled too tightly by Fim1p to allow access by myosin, so that myosin must displace Fim1p as contraction begins. Such displacement has been observed with the *Dictyostelium* proteins in vitro (Prassler *et al.*, 1997). Because α-actinins can bind (directly or indirectly) to membrane proteins (Critchley and Flood, 1999), Ain1p may help to link the medial ring to the plasma membrane during contraction. However, the successful cytokinesis of *ain1* deletion cells under normal conditions shows that this role must also be redundant with that of at least one other protein.

It is not yet known whether either α-actinin or fimbrin functions in cytokinesis in other organisms. Although α-actinins concentrate in the cleavage furrows of some animal cells and a fimbrin concentrates in the cleavage furrow of *Tetrahymena* (see INTRODUCTION), no strong evidence has been obtained to support direct roles for these proteins in cytokinesis in these cell types. Moreover, in *Dictyostelium*, neither α-actinin nor fimbrin is detectably enriched in the cleavage furrow, and no substantial cytokinesis defect has been detected in cells that are lacking either protein (Schleicher *et al.*, 1988; Prassler *et al.*, 1997; Rivero *et al.*, 1999; Weber *et al.*, 1999). Instead, two other actin-bundling proteins, the cortexillins, are enriched in cleavage furrows and required for normal cytokinesis (Faix *et al.*, 1996; Weber *et al.*, 1999). However, it remains possible that a *Dictyostelium* α-actinin-fimbrin double mutant (which has not been described) would have a defect in cytokinesis or that this organism has an additional α-actinin and/or fimbrin that is involved in cytokinesis. In any case, given the conserved role of the actomyosin contractile ring in cytokinesis, the findings in fission yeast raise the possibility that α-actinins and/or fimbrins are involved in organizing this ring also in other organisms.

Roles of Fim1p in Polarized Growth and Sexual Differentiation

Several lines of evidence indicate that in addition to its role in cytokinesis, Fim1p is also important for proper function of the actin cytoskeleton in polarized growth during interphase and the sexual cycle. First, Fim1p localizes in an actin-dependent manner to patches very similar to those of F-actin at the growing cell ends, the cell division site, and the tips of mating projections and germinating spores, as well as around developing spores in the ascus. In addition, *fim1* deletion cells show aberrations in actin patch morphology and distribution, are rounder than wild-type cells, and have mating and sporulation defects. Although the detailed structure and molecular functions of actin patches are not yet understood, they probably function in polarized secretion of cell wall and other cell surface materials (reviewed by Bähler and Peter, 2000). Thus, the data suggest that the actin-bundling activity provided by Fim1p is required for proper actin patch function during both vegetative and sexual development. This role appears similar to that of the *S. cerevisiae* fimbrin Sac6p. However, Sac6p is also involved in actin cable function (Adams *et al.*, 1991), whereas no such role was evident for Fim1p. Fim1p was not detectable in actin cables, and *fim1* deletion cells did not have obvious defects in such cables. However, because these cables are generally more difficult to visualize in *S. pombe* than in *S. cerevisiae,* it is also possible that we failed to detect a subtle role of Fim1p. *sac6* mutants are also defective in the internalization of mating pheromone, suggesting that fimbrin is also involved in endocytosis in *S. cerevisiae* (Kübler and Riezman, 1993). Thus, the mating defect of *fim1* mutants may also be caused, at least in part, by a defect in endocytosis.

Possible Regulation of Ain1p and Fim1p

Because cytokinesis and polarized growth require precise temporal and spatial regulation, it will be important to identify the regulators for Ain1p and Fim1p in vivo. Both proteins have regions with recognizable similarity to EF hands, but none of these regions seems likely to be functional for Ca^{2+} binding (Strynadka and James, 1989), so that neither Ain1p nor Fim1p seems likely to be regulated by Ca^{2+}. α-Actinins have been found to bind phosphatidylinositol 4,5-bisphosphate and to interact with several proteins, including CRP1, integrin, vinculin, and zyxin (Fukami *et al.*, 1996; Pomiès *et al.*, 1997; and references cited therein). Ain1p has one possible phosphatidylinositol 4,5-bisphosphate binding site, and a CRP1 homologue (accession number

Q14014) has been identified by the genome project, so that these elements may be important in the regulation of Ain1p. L-plastin becomes phosphorylated by an unknown kinase when leukocytes are activated by growth factors (Zu *et al.*, 1990), and it is constitutively phosphorylated on serine residues in its EF-hand motifs in adherent macrophages (Messier *et al.*, 1993). Thus, Fim1p may be regulated by protein kinases. Identification and characterization of regulators and/or binding partners for Ain1p and Fim1p should help to elucidate the roles of these proteins in actin function.

ACKNOWLEDGMENTS

We thank Paul Nurse, Jürg Kohli, Dan McCollum, Kathy Gould, Mohan Balasubramanian, Fred Chang, Viesturs Simanis, and Fulvia Verde for strains; Charles Albright, John Fikes, and Paul Young for DNA libraries; Mark Longtine, Erfei Bi, Dan McCollum, and members of our laboratory for valuable discussions; Liz Weaver and Alex Steever for technical assistance; and Susan Whitfield for outstanding photographic services. This work was supported by National Institutes of Health Grant GM-31006.

REFERENCES

Adams, A.E.M., Botstein, D., and Drubin, D.G. (1991). Requirement of yeast fimbrin for actin organization and morphogenesis in vivo. Nature *354*, 404–408.

Adams, A.E.M., Cooper, J.A., and Drubin, D.G. (1993). Unexpected combinations of null mutations in genes encoding the actin cytoskeleton are lethal in yeast. Mol. Biol. Cell *4*, 459–468.

Adams, A.E.M., Shen, W., Lin, C.-S., Leavitt, J., and Matsudaira, P. (1995). Isoform-specific complementation of the yeast *sac6* null mutation by human fimbrin. Mol. Cell. Biol. *15*, 69–75.

Alberts, B., Bray, D., Lewis, J., Raff, M., Roberts, K., and Watson, J.D. (1994). Molecular Biology of the Cell, 3rd edition, New York, New York: Garland Publishing.

Arai, R., Nakano, K., and Mabuchi, I. (1998). Subcellular localization and possible function of actin, tropomyosin and actin-related protein 3 (Arp3) in the fission yeast *Schizosaccharomyces pombe*. Eur. J. Cell Biol. *76*, 288–295.

Ayscough, K.R. (1998). In vivo functions of actin-binding proteins. Curr. Opin. Cell Biol. *10*, 102–111.

Ayscough, K.R., Stryker, J., Pokala, N., Sanders, M., Crews, P., and Drubin, D.G. (1997). High rates of actin filament turnover in budding yeast and roles for actin in establishment and maintenance of cell polarity revealed using the actin inhibitor latrunculin-A. J. Cell Biol. *137*, 399–416.

Bähler, J., and Peter, M. (2000). Cell polarity in yeast. In: Cell Polarity, ed. D. Drubin, Oxford: Oxford University Press, 21–77.

Bähler, J., and Pringle, J.R. (1998). Pom1p, a fission yeast protein kinase that provides positional information for both polarized growth and cytokinesis. Genes Dev. *12*, 1356–1370.

Bähler, J., Steever, A.B., Wheatley, S., Wang, Y., Pringle, J.R., Gould, K.L., and McCollum, D. (1998a). Role of polo kinase and Mid1p in determining the site of cell division in fission yeast. J. Cell Biol. *143*, 1603–1616.

Bähler, J., Wu, J.-Q., Longtine, M.S., Shah, N.G., McKenzie, A., III, Steever, A.B., Wach, A., Philippsen, P., and Pringle, J.R. (1998b). Heterologous modules for efficient and versatile PCR-based gene targeting in *Schizosaccharomyces pombe*. Yeast *14*, 943–951.

Balasubramanian, M.K., Helfman, D.M., and Hemmingsen, S.M. (1992). A new tropomyosin essential for cytokinesis in the fission yeast *S. pombe*. Nature *360*, 84–87.

Balasubramanian, M.K., Hirani, B.R., Burke, J.D., and Gould, K.L. (1994). The *Schizosaccharomyces pombe cdc3*$^{+}$ gene encodes a profilin essential for cytokinesis. J. Cell Biol. *125*, 1289–1301.

Balasubramanian, M.K., McCollum, D., Chang, L., Wong, K.C.Y., Naqvi, N.I., He, X., Sazer, S., and Gould, K.L. (1998). Isolation and characterization of new fission yeast cytokinesis mutants. Genetics *149*, 1265–1275.

Balasubramanian, M.K., McCollum, D., and Gould, K.L. (1997). Cytokinesis in fission yeast *Schizosaccharomyces pombe*. Methods Enzymol. *283*, 494–506.

Bartles, J.R. (2000). Parallel actin bundles and their multiple actin-bundling proteins. Curr. Opin. Cell Biol. *12*, 72–78.

Basi, G., Schmid, E., and Maundrell, K. (1993). TATA box mutations in the *Schizosaccharomyces pombe nmt1* promoter affect transcription efficiency but not the transcription start point or thiamine repressibility. Gene *123*, 131–136.

Becker, D.M., Fikes, J.D., and Guarente, L. (1991). A cDNA encoding a human CCAAT-binding protein cloned by functional complementation in yeast. Proc. Natl. Acad. Sci. USA *88*, 1968–1972.

Bezanilla, M., Forsburg, S.L., and Pollard, T.D. (1997). Identification of a second myosin-II in *Schizosaccharomyces pombe*: Myp2p is conditionally required for cytokinesis. Mol. Biol. Cell *8*, 2693–2705.

Bi, E., Maddox, P., Lew, D.J., Salmon, E.D., McMillan, J.N., Yeh, E., and Pringle, J.R. (1998). Involvement of an actomyosin contractile ring in *Saccharomyces cerevisiae* cytokinesis. J. Cell Biol. *142*, 1301–1312.

Botstein, D., Amberg, D., Mulholland, J., Huffaker, T., Adams, A., Drubin, D., and Stearns, T. (1997). The yeast cytoskeleton. In: The Molecular and Cellular Biology of the Yeast *Saccharomyces*. Cell Cycle and Cell Biology, eds. J.R. Pringle, J.R. Broach, and E.W. Jones, Cold Spring Harbor, NY: Cold Spring Harbor Laboratory Press, 1–90.

Bresnick, A.R., Warren, V., and Condeelis, J. (1990). Identification of a short sequence essential for actin binding by Dictyostelium ABP-120. J. Biol. Chem. *265*, 9236–9240.

Chang, F., Drubin, D., and Nurse, P. (1997). Cdc12p, a protein required for cytokinesis in fission yeast, is a component of the cell division ring and interacts with profilin. J. Cell Biol. *137*, 169–182.

Chang, F., and Nurse, P. (1996). How fission yeast fission in the middle. Cell *84*, 191–194.

Correia, I., and Matsudaira, P. (1999). Fimbrin. In: Guidebook to the Cytoskeletal and Motor Proteins, 2nd edition, eds. T. Kreis and R. Vale, Oxford: Oxford University Press, 97–99.

Critchley, D.R., and Flood, G. (1999). α-Actinins. In: Guidebook to the Cytoskeletal and Motor Proteins, 2nd edition, eds. T. Kreis and R. Vale, Oxford: Oxford University Press, 24–27.

Djinovic-Carugo, K., Young, P., Gautel, M., and Saraste, M. (1999). Structure of the α-actinin rod: molecular basis for cross-linking of actin filaments. Cell *98*, 537–546.

Doyle, T., and Botstein, D. (1996). Movement of yeast cortical actin cytoskeleton visualized *in vivo*. Proc. Natl. Acad. Sci. USA *93*, 3886–3891.

Drenckhahn, D., Engel, K., Höfer, D., Merte, C., Tilney, L., and Tilney, M. (1991). Three different actin filament assemblies occur in every hair cell: each contains a specific actin crosslinking protein. J. Cell Biol. *112*, 641–651.

Drubin, D.G., Miller, K.G., and Botstein, D. (1988). Yeast actin-binding proteins: evidence for a role in morphogenesis. J. Cell Biol. *107*, 2551–2561.

Ebashi, S., and Ebashi, F. (1965). α-Actinin, a new structural protein from striated muscle. I. Preparation and action on actomyosin-ATP interaction. J. Biochem. *58*, 7–12.

Eng, K., Naqvi, N.I., Wong, K.C.Y., and Balasubramanian, M.K. (1998). Rng2p, a protein required for cytokinesis in fission yeast, is a component of the actomyosin ring and the spindle pole body. Curr. Biol. *8*, 611–621.

Faix, J., Steinmetz, M., Boves, H., Kammerer, R.A., Lottspeich, F., Mintert, U., Murphy, J., Stock, A., Aebi, U., and Gerisch, G. (1996). Cortexillins, major determinants of cell shape and size, are actin-bundling proteins with a parallel coiled-coil tail. Cell *86*, 631–642.

Forsburg, S.L. (1993). Comparison of *Schizosaccharomyces pombe* expression systems. Nucleic Acids Res. *21*, 2955–2956.

Fujiwara, K., Porter, M.E., and Pollard, T.D. (1978). Alpha-actinin localization in the cleavage furrow during cytokinesis. J. Cell Biol. *79*, 268–275.

Fukami, K., Sawada, N., Endo, T., and Takenawa, T. (1996). Identification of a phosphatidylinositol 4,5-bisphosphate-binding site in chicken skeletal muscle α-actinin. J. Biol. Chem. *271*, 2646–2650.

Furukawa, R., and Fechheimer, M. (1997). The structure, function, and assembly of actin filament bundles. Int. Rev. Cytol. *175*, 29–90.

Fyrberg, E., Kelly, M., Ball, E., Fyrberg, C., and Reedy, M.C. (1990). Molecular genetics of *Drosophila* alpha-actinin: mutant alleles disrupt Z disc integrity and muscle insertions. J. Cell Biol. *110*, 1999–2011.

Gould, K.L., and Simanis, V. (1997). The control of septum formation in fission yeast. Genes Dev. *11*, 2939–2951.

Hales, K.G., Bi, E., Wu, J.-Q., Adam, J.C., Yu, I.-C., and Pringle, J.R. (1999). Cytokinesis: an emerging unified theory for eukaryotes? Curr. Opin. Cell Biol. *11*, 717–725.

Hiraoka, Y., Toda, T., and Yanagida, M. (1984). The *NDA3* gene of fission yeast encodes β-tubulin: a cold-sensitive *nda3* mutation reversibly blocks spindle formation and chromosome movement in mitosis. Cell *39*, 349–358.

Höfer, D., and Drenckhahn, D. (1996). Cytoskeletal differences between stereocilia of the human sperm passageway and microvilli/stereocilia in other locations. Anat. Rec. *245*, 57–64.

Jockusch, B.M., Zurek, B., Zahn, R., Westmeyer, A., and Füchtbauer, A. (1991). Antibodies against vertebrate microfilament proteins in the analysis of cellular motility and adhesion. J. Cell Sci. Suppl. *14*, 41–47.

Kitayama, C., Sugimoto, A., and Yamamoto, M. (1997). Type II myosin heavy chain encoded by the *myo2* gene composes the contractile ring during cytokinesis in *Schizosaccharomyces pombe*. J. Cell Biol. *137*, 1309–1319.

Kübler, E., and Riezman, H. (1993). Actin and fimbrin are required for the internalization step of endocytosis in yeast. EMBO J. *12*, 2855–2862.

Leupold, U. (1970). Genetical methods for *Schizosaccharomyces pombe*. Methods Cell Physiol. *4*, 169–177.

Lin, C.-S., Aebersold, R.H., Kent, S.B., Varma, M., and Leavitt, J. (1988). Molecular cloning and characterization of plastin, a human leukocyte protein expressed in transformed human fibroblasts. Mol. Cell. Biol. *8*, 4659–4668.

Lin, C.-S., Aebersold, R.H., and Leavitt, J. (1990). Correction of the N-terminal sequences of the human plastin isoforms by using anchored polymerase chain reaction: identification of a potential calcium-binding domain. Mol. Cell. Biol. *10*, 1818–1821.

Lippincott, J., and Li, R. (1998). Sequential assembly of myosin II, an IQGAP-like protein, and filamentous actin to a ring structure involved in budding yeast cytokinesis. J. Cell Biol. *140*, 355–366.

Mabuchi, I., Hamaguchi, Y., Kobayashi, T., Hosoya, H. Tsukita, S., and Tsukita, S. (1985). Alpha-actinin from sea urchin eggs: biochemical properties, interaction with actin, and distribution in the cell during fertilization and cleavage. J. Cell Biol. *100*, 375–383.

Marks, J., and Hyams, J.S. (1985). Localization of F-actin through the cell division cycle of *Schizosaccharomyces pombe*. Eur. J. Cell Biol. *39*, 27–32.

Matsudaira, P. (1994a). Actin crosslinking proteins at the leading edge. Semin. Cell Biol. *5*, 165–174.

Matsudaira, P. (1994b). The fimbrin and alpha-actinin footprint on actin. J. Cell Biol. *126*, 285–287.

Maundrell, K. (1990). *nmt1* of fission yeast. A highly transcribed gene completely repressed by thiamine. J. Biol. Chem. *265*, 10857–10864.

May, K.M., Watts, F.Z., Jones, N., and Hyams, J.S. (1997). Type II myosin involved in cytokinesis in the fission yeast, *Schizosaccharomyces pombe*. Cell Motil. Cytoskeleton *38*, 385–396.

McCollum, D., Balasubramanian, M.K., Pelcher, L.E., Hemmingsen, S.M., and Gould, K.L. (1995). *Schizosaccharomyces pombe cdc4*$^{+}$ gene encodes a novel EF-hand protein essential for cytokinesis. J. Cell Biol. *130*, 651–660.

McCollum, D., Feoktistova, A., Morphew, M., Balasubramanian, M., and Gould, K.L. (1996). The *Schizosaccharomyces pombe* actin-related protein, Arp3, is a component of the cortical actin cytoskeleton and interacts with profilin. EMBO J. *15*, 6438–6446.

Messier, J.M., Shaw, L.M., Chafel, M., Matsudaira, P., and Mercurio, A.M. (1993). Fimbrin localized to an insoluble cytoskeletal fraction is constitutively phosphorylated on its headpiece domain in adherent macrophages. Cell Motil. Cytoskeleton *25*, 223–233.

Meyer, R.K., and Aebi, U. (1990). Bundling of actin filaments by α-actinin depends on its molecular length. J. Cell Biol. *110*, 2013–2024.

Millake, D.B., Blanchard, A.D., Patel, B., and Critchley, D.R. (1989). The cDNA sequence of a human placental α-actinin. Nucleic Acids Res. *17*, 6725.

Minet, M., Nurse, P., Thuriaux, P., and Mitchison, J.M. (1979). Uncontrolled septation in a cell division cycle mutant of the fission yeast *Schizosaccharomyces pombe*. J. Bacteriol. *137*, 440–446.

Mitchison, J.M., and Nurse, P. (1985). Growth in cell length in the fission yeast *Schizosaccharomyces pombe*. J. Cell Sci.*75*, 357–376.

Moreno, S., Klar, A., and Nurse, P. (1991). Molecular genetic analysis of fission yeast *Schizosaccharomyces pombe.* Methods Enzymol. *194*, 795–823.

Motegi, F., Nakano, K., Kitayama, C., Yamamoto, M., and Mabuchi, I. (1997). Identification of Myo3, a second type-II myosin heavy chain in the fission yeast *Schizosaccharomyces pombe*. FEBS Lett. *420*, 161–166.

Naqvi, N.I., Eng, K., Gould, K.L., and Balasubramanian, M.K. (1999). Evidence for F-actin-dependent and -independent mechanisms involved in assembly and stability of the medial actomyosin ring in fission yeast. EMBO J. *18*, 854–862.

Noegel, A., Witke, W., and Schleicher, M. (1987). Calcium-sensitive non-muscle α-actinin contains EF-hand structures and highly conserved regions. FEBS Lett. *221*, 391–396.

Nurse, P. (1994). Fission yeast morphogenesis - posing the problems. Mol. Biol. Cell *5*, 613–616.

Nurse, P., Thuriaux, P., and Nasmyth, K. (1976). Genetic control of the cell division cycle in the fission yeast *Schizosaccharomyces pombe*. Mol. Gen. Genet. *146*, 167–178.

Otto, J.J. (1994). Actin-bundling proteins. Curr. Opin. Cell Biol. *6*, 105–109.

Pascual, J., Castresana, J., and Saraste, M. (1997). Evolution of the spectrin repeat. BioEssays *19*, 811–817.

Petersen, J., Nielsen, O., Egel, R., and Hagan, I.M. (1998). F-actin distribution and function during sexual differentiation in *Schizosaccharomyces pombe*. J. Cell Sci. *111*, 867–876.

Pomiès, P., Louis, H.A., and Beckerle, M.C. (1997). CRP1, a LIM domain protein implicated in muscle differentiation, interacts with α-actinin. J. Cell Biol. *139*, 157–168.

Prabhala, G., Rosenberg, G.H., and Käufer, N.F. (1992). Architectural features of pre-mRNA introns in the fission yeast *Schizosaccharomyces pombe*. Yeast 8, 171–182.

Prassler, J., Stocker, S., Marriott, G., Heidecker, M., Kellermann, J., and Gerisch, G. (1997). Interaction of a *Dictyostelium* member of the plastin/fimbrin family with actin filaments and actin-myosin complexes. Mol. Biol. Cell *8*, 83–95.

Pruyne, D., and Bretscher, A. (2000). Polarization of cell growth in yeast. II. The role of the cortical actin cytoskeleton. J. Cell Sci. *113*, 571–585.

Rivero, F., Furukawa, R., Fechheimer, M., and Noegel, A.A. (1999). Three actin cross-linking proteins, the 34 kDa actin-bundling protein, α-actinin and gelation factor (ABP-120), have both unique and redundant roles in the growth and development of *Dictyostelium*. J. Cell Sci. *112*, 2737–2751.

Rivero, F., Köppel, B., Peracino, B., Bozzaro, S., Siegert, F., Weijer, C.J., Schleicher, M., Albrecht, R., and Noegel, A.A. (1996). The role of the cortical cytoskeleton: F-actin crosslinking proteins protect against osmotic stress, ensure cell size, cell shape and motility, and contribute to phagocytosis and development. J. Cell Sci. *109*, 2679–2691.

Roulier, E.M., Fyrberg, C., and Fyrberg, E. (1992). Perturbations of *Drosophila* α-actinin cause muscle paralysis, weakness, and atrophy but do not confer obvious nonmuscle phenotypes. J. Cell Biol. *116*, 911–922.

Sambrook, J., Fritsch, E.F., and Maniatis, T. (1989). Molecular Cloning: A Laboratory Manual, Cold Spring Harbor, NY: Cold Spring Harbor Laboratory Press.

Sanger, J.M., Mittal, B., Pochapin, M.B., and Sanger, J.W. (1987). Stress fiber and cleavage furrow formation in living cells microinjected with fluorescently labeled α-actinin. Cell Motil. Cytoskeleton *7*, 209–220.

Sawin, K.E., and Nurse, P. (1998). Regulation of cell polarity by microtubules in fission yeast. J. Cell Biol. *142*, 457–471.

Schleicher, M., Noegel, A., Schwarz, T., Wallraff, E., Brink, M., Faix, J., Gerisch, G., and Isenberg, G. (1988). A *Dictyostelium*. mutant with severe defects in α-actinin: its characterization using cDNA probes and monoclonal antibodies. J. Cell Sci. *90*, 59–71.

Sohrmann, M., Fankhauser, C., Brodbeck, C., and Simanis, V. (1996). The *dmf1/mid1* gene is essential for correct positioning of the division septum in fission yeast. Genes Dev. *10*, 2707–2719.

Strynadka, N.C.J., and James, M.N.G. (1989). Crystal structures of the helix-loop-helix calcium-binding proteins. Annu. Rev. Biochem. *58*, 951–998.

Tilney, L.G., Connelly, P.S., Vranich, K.A., Shaw, M.K., and Guild, G.M. (1998). Why are two different cross-linkers necessary for actin bundle formation in vivo and what does each cross-link contribute? J. Cell Biol. *143*, 121–133.

Vallen, E.A., Caviston, J., and Bi, E. (2000). Roles of Hof1p, Bni1p, Bnr1p, and Myo1p in cytokinesis in *Saccharomyces cerevisiae*. Mol. Biol. Cell *11*, 593–611.

Watanabe, A., Kurasawa, Y., Watanabe, Y., and Numata, O. (1998). A new *Tetrahymena* actin-binding protein is localized in the division furrow. J. Biochem. *123*, 607–613.

Watanabe, A., Yonemura, I., Gonda, K., and Numata, O. (2000). Cloning and sequencing of the gene for a *Tetrahymena* fimbrin-like protein. J. Biochem. *127*, 85–94.

Weber, I., Gerisch, G., Heizer, C., Murphy, J., Badelt, K., Stock, A., Schwartz, J.-M., and Faix, J. (1999). Cytokinesis mediated through the recruitment of cortexillins into the cleavage furrow. EMBO J. *18*, 586–594.

Wright, A., Maundrell, K., Heyer, W.-D., Beach, D., and Nurse, P. (1986). Vectors for the construction of gene banks and the integration of cloned genes in *Schizosaccharomyces pombe* and *Saccharomyces cerevisiae*. Plasmid *15*, 156–158.

Zu, Y., Shigesada, K., Nishida, E., Kubota, I., Kohno, M., Hanaoka, M., and Namba, Y. (1990). 65-kilodalton protein phosphorylated by interleukin 2 stimulation bears two putative actin-binding sites and two calcium-binding sites. Biochemistry *29*, 8319–8324.